Measurement of the Dynamic Bulk Compliance of Polymers

Thesis by

Tony H. Deng

In Partial Fulfillment of the Requirements

for the Degree of

Doctor of Philosophy

Graduate Aeronautical Laboratories

California Institute of Technology

Pasadena, California

1997

(Submitted January 3, 1997)

to my family

Acknowledgements

I would like to thank Dr. Wolfgang Knauss, Professor of Aeronautics, for his supervision and patience during the course of this research. I also would like to thank Professors Knowles, Caughey, Sturtevant, Ravichandran, and Rosakis for their guidance through courses and conversations during my stay in Caltech. I must offer special thanks to Professors Brennen, Iwan, Ravichandran and Goodwin for taking their time to serve on my Ph.D. thesis committee.

I wish to thank Dr. Carl Shultheisz for the initial design of the pressure chamber used in this project. I am grateful to Professor Wilson Nolle of University of Texas, Austin, for the advice on pressure chamber design; Professor Tanaka of Tokyo University for providing information on piezoelectric charge amplifiers.

This work was initially supported by ONR grant N00014-91-J-1427 with Dr. Peter Schmidt as the monitor, and later work was supported by NASA under grant #NSG 1483 and #NAG 1-1780, with Dr. Tom Gates as the technical monitor. In addition funds from the National Science Foundation under grant #CMS9504144 allowed completion of this study. Their support is gratefully acknowledged.

This thesis is dedicated to my parents in recognition of their love and support throughout all these years.

Finally I express my gratitude and love to my wife Eve for her support and tolerance.

Abstract

Measurements are described and analyzed for the determination of the dynamic bulk compliance for poly(vinyl acetate) [PVAc] as a function of frequency and temperature. The real and imaginary parts of the dynamic bulk compliance over the frequency range from 10 Hz to 1,000 Hz have been measured at different temperatures by determining the compressibility of a specimen confined to an oil-filled cavity via pressurization by a piezoelectric driver and response of a piezoelectric sensor. The wavelength of the compressional wave generated by the piezoelectric transducer over the frequency range used is much larger than the size of the cavity so that the pressure can be considered uniform inside the cavity. The complex compliances of the specimen, confining liquid, and the cavity, are additive upon the pressure variations due to the piezoelectric transducer expansion and contraction. All deformations are considered to be purely dilitational.

A master compliance curve over a total frequency range of about 12 decades is generated by the method of time-temperature superposition. Experimental problems addressing limitations in resolution capability are discussed. The results are compared with the classical measurements obtained by McKinney and Belcher over thirty years ago. Further comparison of the bulk with shear compliance data shows that the extent of the transition ranges for the shear and for the bulk functions are comparable, but the two transitions belong to different time scales: That of the bulk response falls mostly into the glassy domain of the shear behavior. One concludes thus that for linearly viscoelastic response the molecular mechanisms contributing to shear and bulk deformations have different conformational sources.

Contents

List of Figures

List of Tables

Chapter 1 Introduction

1.1 Motivation

The theory of linear viscoelasticity has been formulated and used for several decades along with the identification of the requisite material functions. There are many polymer systems for which relaxation or creep data for either uniaxial or shear response have been measured, and their number is too large to warrant even a partial listing here. By contrast, during this time span the determination of the time dependent bulk (volumetric) response has been surprisingly limited to essentially a single investigation [McKinney and Belcher, 1963] which covers a similarly large time or frequency range. This exceedingly sparse set of investigations into the bulk behavior of polymers is not so much the consequence of relative unimportance, as it is of the extreme difficulties associated with making sufficiently precise measurements of very small deformations. One particular question surrounding the work of McKinney and Belcher is the normally low glass transition temperature reported for their material: While that temperature is usually recorded as being around 30°C McKinney and Belcher determined this value as 16.9°C. Their material may have been a specially compounded PVAc.

The result of the McKinney and Belcher investigation showed that the magnitude of the bulk response changes by a much smaller factor through the transition range as compared to a factor of one hundred to a thousand for the uniaxial or shear behavior, excluding the long-term flow region for uncrosslinked polymers. These findings have been confirmed qualitatively by Lin & Nolle [1989] who measured the bulk response by a nearly identical method, but essentially only as a function of the temperature, inasmuch as the frequency range was very small. Similar measurements over six decades of frequencies but only at room temperature on 42 different polymers by Heydemann [1959] established typically very small variations or constancy of bulk response for these limited conditions (since no transition behavior was included by

choice of the test condition).

In applications of the linear theory of viscoelasticity to engineering problems the limited knowledge of time dependent bulk response has not been a severe impediment inasmuch as the assumptions of a constant bulk modulus has served (engineering) analysts well. However, more recent studies addressing nonlinearly viscoelastic behavior have pointed to the potential need for a more careful characterization of bulk response. Specifically, it has been demonstrated that the dilatational behavior of polymers can have a significant effect on the time dependent shear or uniaxial response once the small deformation range (strains less than about 0.2%) is exceeded. It appears that outside of this small strain range the mutual independence of bulk and shear response ceases, and initial (free volume) models pointed to the need to better understand the bulk response throughout the transition range [Knauss & Emri, 1981; Knauss & Emri, 1987; Losi and Knauss, 1992]. Also studies on nonlinearly viscoelastic behavior involving the interdependency of dilatational and shear deformations on time dependent response reinforced that observation [Duran and McKenna, 1990], though in other studies the nonlinearly viscoelastic behavior has been found to involve an intrinsically nonlinear shear component in addition to the coupling between the volumetric and shear effects [Lu & Knauss, 1996].

In this thesis the issues of polymer viscosity and bulk modulus measurements are first discussed in chapter 1. The measurement of time dependent bulk response is then delineated by describing first the experimental apparatus, along with issues requiring special attention in the pursuit of similar studies in chapter 2. In chapter 3, results of the measurements are recorded and compared with those of McKinney and Belcher, as well as with the transition range for the shear response of the same material, including the time-temperature shift factors for the two deformation modes. A summary in chapter 4 forms the conclusion.

1.2 Viscoelastic Behavior of Polymers

The use of synthetic polymers has increased dramatically in the past two decades. Plastics today play a significant role in all branches of industry. In many situations, manufacturers prefer plastic materials over metals because they are light weight, chemically resistant and easy to manufacture into parts. Polymers are not only widely used as packaging or decorating materials, but also increasingly in load-bearing applications, as, for example, in composites, when polymers form the matrix material re-enforced by stiff fibers. The design of these load-bearing structures of polymers must depend on the accurate and meaningful material data over the entire range of temperature and time scales for which the applications are intended.

Polymers are constructed of molecules containing many repeat units of one or more (low-molecular-weight) "monomers." Polymers typically have very high molecular weights and can be formed by "linear" molecule chains or "cross-linked" networks. Accordingly, polymeric materials are generally grouped into thermo-plastics and thermosets (including elastomers). Thermo-plastics are further separated into crystalline and amorphous solids.

Polymeric materials are noticeably different from classical engineering materials (metals, ceramics, etc) in that they exhibit strong dependence on time and temperature in virtually all of their physical properties. Metals and ceramics can also exhibit creep and stress relaxation; their elastic properties can also vary with temperature. However, because of the weak van der Waals' binding forces involved in inter and intra-chain interactions, polymers show time and temperature effects at much lower stress levels and over smaller temperature ranges.

1.2.1 Linear Viscoelasticity

In classical mechanics the infinitesimal deformation of solid materials is described by Hooke's law, in which, the stress is always linearly proportional to strain but independent on the rate of strain. In classical hydrodynamics the flow of viscous liquids is described by Newton's law, in which the stress is always proportional to

strain rate but independent on the strain itself. However, many materials exhibits viscoelastic behavior, for which stress is dependent both on strain and strain rate.

If the strain is infinitesimal, the time-dependent stress-strain relations can be described by linear differential equations with constant coefficients or convolution integrals, which form the basis of linearly viscoelastic behavior. Then, in a given experiment the ratio of stress to strain is a function of time (or frequency) only, and not of stress amplitude.

By superposition with respect to strain amplitude and time, the constitutive relation of linear viscoelasticity can be written as [Flugge, 1975]

$$\sigma_{ij}(t) = \int_{-\infty}^{t} 2G(t-\tau)\frac{d\epsilon'_{ij}(\tau)}{d\tau}d\tau + \delta_{ij}\int_{-\infty}^{t} K(t-\tau)\frac{d\epsilon_{kk}(\tau)}{d\tau}d\tau, \tag{1.1}$$

where $G(t)$ and $K(t)$ are the time-dependent shear and bulk moduli, respectively, and

$$\epsilon'_{ij} = \epsilon_{ij} - \frac{1}{3}\delta_{ij}\epsilon_{kk} \tag{1.2}$$

represents the deviatoric part of the strain tensor.

In linear viscoelasticity, $G(t)$ and $K(t)$ are independent of each other. Extensional viscosity deals with small deformation state between solid and liquid, uncrosslinked flow, and nonlinear range.

When "perceptible" changes in volume occur, both $G(t)$ and $K(t)$ are found to depend strongly on the degree of compression or dilatation. Hence linear behavior must be limited to extremely small volume changes. [Ferry, 1980]

1.2.2 Volume Relaxation of Polymers

Consider a body of isotropic and homogeneous viscoelastic material under uniformly hydrostatic pressure,

$$\sigma_{11} = \sigma_{22} = \sigma_{33} = P(t), \sigma_{12} = \sigma_{23} = \sigma_{31} = 0. \tag{1.3}$$

Then equation (1.1) becomes

$$P(t) = \int_{-\infty}^{t} K(t-\tau)\frac{\epsilon_{kk}(\tau)}{d\tau}d\tau, \tag{1.4}$$

So that a relaxation experiment, for which

$$\epsilon_{kk} = \epsilon_{kk}^{o} h(t) \tag{1.5}$$

($h(t)$ is the unit Heaviside function) leads to

$$P(t) = \epsilon_{kk}^{o} K(t). \tag{1.6}$$

On the other hand, if the pressure $P = P_o h(t)$ is applied and the volume change is traced as a function of time, the bulk creep response is described by,

$$\epsilon_{kk} = P_o M(t) \tag{1.7}$$

where $M(t)$ is the bulk creep compliance.

The relationship between bulk relaxation modulus $K(t)$ and bulk creep compliance $M(t)$ can be expressed as

$$\int_0^t K(\tau)M(t-\tau)d\tau = t. \tag{1.8}$$

Alternatively, the strain may be varied periodically, and specifically, with a sinusoidal variation. For linearly viscoelastic behavior, the stress will also alternate sinusoidally but will be out of phase with the strain. This can be shown from the constitutive equations as follows. Let

$$\epsilon_{kk}(t) = \epsilon_o \sin(\omega t) \tag{1.9}$$

where ϵ_o is the maximum amplitude of the strain. Then

$$\frac{d\epsilon_{kk}(t)}{dt} = \omega\epsilon_o \cos(\omega t). \tag{1.10}$$

Substituting into equation (1.4), one has, after all transients have died out

$$P(t) = \int_{-\infty}^{t} K(t-\tau)\omega\epsilon_o \cos(\omega\tau)d\tau. \tag{1.11}$$

Let $\xi = t - \tau$, we have then

$$\begin{aligned} P(t) &= \int_0^{\infty} K(\xi)\omega\epsilon_o \cos[\omega(t-\xi)]d\xi \\ &= \epsilon_o \left[\omega \int_0^{\infty} K(\xi)\sin(\omega\xi)d\xi\right] \sin(\omega t) \\ &\quad +\epsilon_o \left[\omega \int_0^{\infty} K(\xi)\cos(\omega\xi)d\xi\right] \cos(\omega t). \end{aligned} \tag{1.12}$$

It is clear that the term in $\sin(\omega t)$ is in phase with the strain and the term in $\cos(\omega t)$ is 90^o out of phase.

Define,

$$K^{'}(\omega) = \omega \int_0^{\infty} K(\xi)\sin(\omega\xi)d\xi, \tag{1.13}$$

$$K^{''}(\omega) = \omega \int_0^{\infty} K(\xi)\cos(\omega\xi)d\xi. \tag{1.14}$$

So that

$$P(t) = \epsilon^o[K^{'}(\omega)\sin(\omega t) + K^{''}(\omega)\cos(\omega t)]. \tag{1.15}$$

The frequency dependent functions $K^{'}(\omega)$ and $K^{''}(\omega)$ are called the bulk storage modulus and bulk loss modulus, respectively.

It is sometimes convenient to express the sinusoidally varying stress and strain as complex quantities. Then the modulus is also complex, given by

$$\frac{\sigma^*}{\epsilon^*} = K^*(\omega) = K^{'}(\omega) + iK^{''}(\omega), \tag{1.16}$$

$$|K^*(\omega)| = \frac{\sigma_o}{\epsilon_o} = \sqrt{K^{'2}(\omega) + K^{''2}(\omega)}. \tag{1.17}$$

The data from sinusoidal experiments can also be expressed in terms of a complex

compliance

$$M^*(\omega) = M'(\omega) - iM''(\omega), \tag{1.18}$$

$$|M^*(\omega)| = \frac{\epsilon_o}{\sigma_o} = \sqrt{M'^2(\omega) + M''^2(\omega)}. \tag{1.19}$$

The storage modulus $K'(\omega)$ and compliance $M'(\omega)$ are so named because they are directly proportional to the average energy storage in a deformation cycle. The loss modulus $K''(\omega)$ and compliance $M''(\omega)$ are directly proportional to the average dissipation or loss of energy as heat in a deformation cycle.

Since $M^*(\omega) = 1/K^*(\omega)$, their individual components are related by the following equations:

$$M'(\omega) = \frac{K'(\omega)}{K'^2(\omega) + K''^2(\omega)}, \tag{1.20}$$

$$M''(\omega) = \frac{K''(\omega)}{K'^2(\omega) + K''^2(\omega)}, \tag{1.21}$$

$$K'(\omega) = \frac{M'(\omega)}{M'^2(\omega) + M''^2(\omega)}, \tag{1.22}$$

$$K''(\omega) = \frac{M''(\omega)}{M'^2(\omega) + M''^2(\omega)}. \tag{1.23}$$

Shear and bulk complex moduli and compliances are measured under cyclic excitation, in what is called "dynamic testing." A given experimental method may cover only 2 to 3 decades in frequency. In order to obtain material properties over many decades, results of measurement from different methods have to be combined or experiments are conducted at different temperatures. The measured data at different temperatures can then be shifted to cover a much wider frequency range according to the time-temperature superposition principle, which will be discussed in the next section.

1.2.3 Time-Temperature Superposition

For many polymers measurements have shown that higher temperatures induce faster relaxation or creep than lower temperatures. The time-temperature superposition, or reduced variable method, is a technique that enables one to shift the experimental curves of different temperatures along the logarithm time or frequency axis to form a "master curve." This enlarges the range of available time or frequency much beyond the range of isothermal measurements. The principle of time-temperature superposition was first observed by Leaderman [1943] who found that in creep measurements a superposition of isothermal curves could be obtained by shifting them on a logarithmic time axis. Tobolsky and Andrews [1943] elaborated on this idea and introduced a change of the modulus due to volume and absolute temperature for stress relaxation measurements. Using time-temperature superposition, a curve measured in the range of 2-3 decades of experimental frequencies can be shifted together to give 10-12 decades of reduced frequency [Fitsgerald and Ferry, 1953], proving the enormous value of the method for the investigation of viscoelastic properties.

Mathematically the curve shifting can be expressed as

$$J(T,t) = J(T_o, t/a_T), \tag{1.24}$$

where the effect of changing temperature is the same as applying a multiplicative factor to the time scale, i.e., and additive factor to the log time (or frequency) scale. a_T in the above equation is a function of temperature and is called the shift factor. Vertical shift is also required to account for rubber elasticity and thermal expansion effects. Tobolsky [1943] proposed to multiply each $J(t)$ value by the ratio $T\rho/T_o\rho_o$, where T_o, ρ_o are the reference temperature and density at that temperature and T, ρ the same quantities for data being modified. The ratio T/T_o in the above compensates for the change in terminal modulus in the rubbery material (where rubber elasticity theory predicts that the shear modulus $G \propto T$) while the density ratio arises from thermal expansion.

Based on the experimental curves of $\log a_T$ of shear compliance versus temperature

for a large number of systems, Williams, Landel & Ferry (1955) found experimentally that $\log a_T$ followed a relation of the form (WLF equation)

$$\log a_T = \frac{-C_1(T - T_g)}{C_2 + T - T_g}, \tag{1.25}$$

where C_1 and C_2 are complex constants, T_g is the glass transition temperature of the polymer. C_1 and C_2, originally thought to be universal constants were found to have different values for different polymers.

1.2.4 Free Volume Theory

The free volume concept was introduced by Batchinski [1913] and later further developed by Doolittle [1951]. They suggested that the resistance to flow of a liquid depended on the free space available to a molecule. Williams, Landel & Ferry [1955] adapted Doolittle's theory for low-molecular weight liquids to the case of high molecular weight polymers.

It is difficult to define free volume (as free space between molecules) in a precise quantitatively manner, especially for high molecular weight polymers. In an approximate way we can represent the segments of a polymer chain by rigid bodies and the free volume as the holes present between these segments as a result of packing requirements. The total volume of a polymer is considered as the sum of the free volume v_f and an occupied volume v_o. The occupied volume v_o includes not only the volume of molecular chains but also the volume associated with vibrational motion. Therefore the free volume is the extra volume required for larger-scale vibrational motions than those found between consecutive atoms of the same chain.

The glass transition temperature T_g is defined on the free volume concept as that temperature at which v_f collapses to zero, or at any rate to a frozen-in value. Polymer molecular chain mobility has therefore been totally restricted and the only movement below T_g is that allowed by the occupied volume v_o.

The WLF equation was derived on the basis of free volume concepts.

$$\log a_T = \frac{B}{2.303}(\frac{1}{f_T} - \frac{1}{f_{T_o}}), \tag{1.26}$$

where f_T and f_{T_o} are the fractional free volume at temperature T and reference temperature T_o. This equation is called Doolittle equation [1951]. B is experimentally found to be close to 1.

The relationship between free volume and temperature can be written as,

$$f = \begin{cases} f_g + \alpha(T - T_g), & T \geq T_g \\ f_g, & T < T_g, \end{cases} \tag{1.27}$$

where the fractional free volume reaches a constant value, f_g, at T_g and increases linearly above T_g. α_f is the coefficient of thermal expansion of the free volume.

The idea of free volume model was further extended to include the effects of strain level and solvent concentration [Knauss & Emri, 1981, 1987; Losi & Knauss, 1992],

$$f = \alpha_f \Delta T + \beta_f \Delta \epsilon_{kk} + \gamma_f \Delta c, \tag{1.28}$$

where ΔT, $\Delta \epsilon_{kk}$, Δc represent the changes in temperature, dilatational strain and solvent concentration. α_f, β_f and γ_f are material properties.

The governing equation for non-linear viscoelastic material is written as

$$\begin{aligned} \sigma_{ij} &= \int_{-\infty}^{t} 2G(\zeta(t) - \zeta(\tau)) \frac{\partial \epsilon'_{ij}(\tau)}{\partial \tau} d\tau \\ &+ \int_{-\infty}^{t} K(\zeta(t) - \zeta(\tau)) \frac{\partial \epsilon_{kk}}{\partial \tau} d\tau, \end{aligned} \tag{1.29}$$

where $G(t)$ and $K(t)$ are the time-dependent shear and bulk moduli, ϵ'_{ij} the deviatoric part of the strain tensor. $\zeta(t)$ represents the internal time of the material,

$$\zeta(t) = \int_0^t \frac{d\tau}{a_T(f(t))}. \tag{1.30}$$

1.3 Bulk Measurement of Polymers

Like time-dependent shear modulus, time-dependent bulk modulus is an important material property for viscoelastic study of polymers. However, bulk modulus are often considered constant (time-independent) because of the difficulties of its measurement. A typical approximation is to assume the Poisson's ratio to be 0.3 and 0.5 respectively for glassy and rubbery state of polymers. Recent studies shows more accurate descriptions are needed for the volume change of polymers due to the nonlinear relationship between the volumetric and shear deformations.

In principle time-dependent bulk modulus can be calculated from time-dependent shear and Young's moduli. However, the method is unfavorable for achieving reliable results, especially for polymers near the rubbery state. The difficulties involved with calculating bulk modulus from shear modulus and Young's modulus can be illustrated through a simple demonstration in terms of linear elasticity [Lu and Knauss, 1996].

The bulk modulus K is expressed in terms of shear modulus G and Young's modulus E,

$$K = \frac{GE}{3(3G - E)}. \tag{1.31}$$

Then,

$$\frac{\Delta K}{K} = \frac{3}{1-2\nu}\frac{\Delta E}{E} - \frac{2(1+\nu)}{1-2\nu}\frac{\Delta G}{G}, \tag{1.32}$$

where ν represents Poisson's ratio.

Therefore,

$$|\frac{\Delta K}{K}| \leq \frac{3}{1-2\nu}|\frac{\Delta E}{E}| + \frac{2(1+\nu)}{1-2\nu}|\frac{\Delta G}{G}|. \tag{1.33}$$

Figure 1.1 shows the percentage error in bulk modulus if calculated from shear and Young's moduli. The percentage error in shear and Young's moduli are assumed to be the same. It is seen from the figure that the error in the bulk modulus is much larger than the percentage error in shear or Young's modulus. For example,

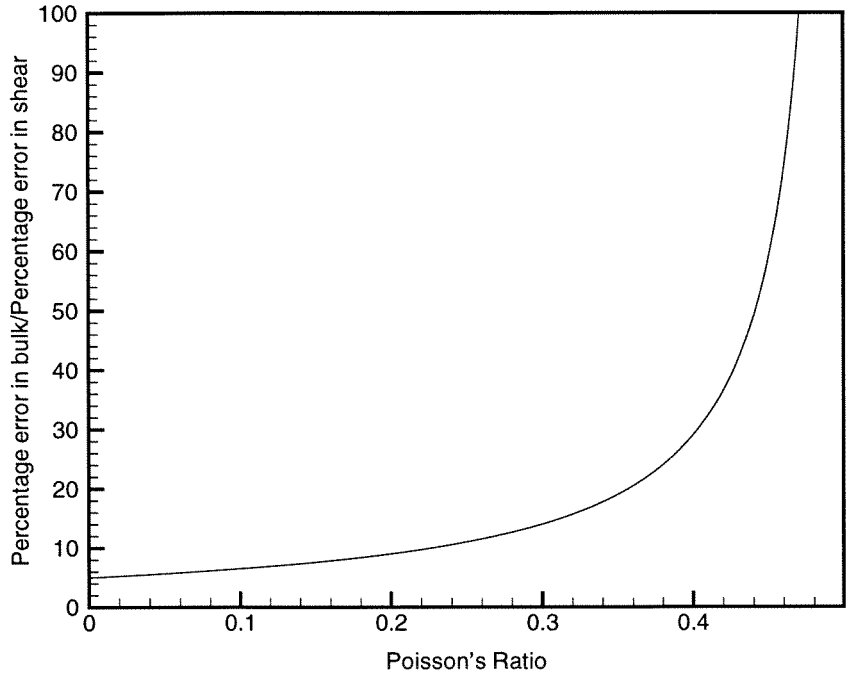

Figure 1.1: Percentage error in the bulk modulus

when $\nu = 0.3$, the percentage error in bulk modulus is 14 times the error in shear or Young's modulus. When Poisson's ratio ν gets close to 0.5, the ratio tends to infinity. The subtraction method involving shear and Young's modulus method is obviously not a favorable method to determine the bulk modulus, especially for large Poisson's ratio values. Thus there is a need to measure bulk modulus directly. In the following sections, different approaches for the measurement of time-dependent bulk modulus are discussed on their advantages and disadvantages.

1.3.1 Transient Bulk Measurement

In the bulk relaxation measurement, one would need to impose a step function of volume change and measure the accompanying pressure as a function of time. Because of the difficulties of measuring this function directly, experiments were instead conducted employing a constant rate of volume decrease. The stress relaxation function

is related to the constant volume changing rate and pressure as a function of time as follows,

$$K(t) = \frac{dP(t)/dt}{d\Delta_v/dt}, \tag{1.34}$$

where $d\Delta_v/dt$ represents the imposed (constant) fractional rate of volume decrease, $P(t)$ the resulting pressure measured from the time the volume change is initiated, and $K(t)$ the stress relaxation modulus. Matsuoka and Maxwell [1958] measured the dilatational stress relaxation modulus through this relation. Their pressure chamber was designed to operate with commercially available testing equipment. The force applied to the plungers was measured as a function of the displacement which was imposed at a constant rate. The deformation of polymer materials generated in this device is not pure volumetric deformation, but a one-dimensional compression with displacement constraint on the other two directions. Matsuoka's results for polystyrene, an amorphous polymer, showed evidence of a glass transition region.

1.3.2 Ultrasonic Wave Measurement

One way to measure bulk modulus is using steady-state wave propagation. [Nolle & Sieck, 1952; Koppelmann, 1955; Wada, *et al*, 1959; Waterman, 1963] The method itself cannot provide a direct measure of the dilatational modulus, but must be evaluated from measurement of two types of waves, generally longitudinal and shear waves. When longitudinal waves are propagated through a thin sheet of polymeric material, the wave propagation is governed by the complex modulus combination L^*,

$$L^* = K^* + \frac{4}{3}G^*. \tag{1.35}$$

Direct measurements of velocity and attenuation are often made with a train of pulses which is sufficiently long to approximate steady-state oscillating deformation at the chosen frequency. A liquid is used as a transmission medium between the ultrasonic transducer and the polymer specimen. Measurements are made first with, then without, a sample of polymer inserted in the wave path through the liquid,

determining the changes in amplitude and phase of a signal echoed back from a reflector or of a signal sent from a transmitter to a receiver. Since the measurement gives the difference between the bulk longitudinal properties of the polymer and the liquid, the latter must be known. The liquid medium has the advantage that no is required to establish mechanical coupling, but the liquid must be chosen carefully to avoid swelling the polymer even to a slight extent and thereby modifying the mechanical properties of the specimen. The frequency range for such measurement is from about 0.5 to 5 MHz.

The attenuation required for determining the viscous component of a modulus association with propagation of a wave are difficult to measure precisely, so that the determination of a bulk modulus which involves the difference between two such quantities is subject to a considerable uncertainty.

1.3.3 Dynamic Bulk Measurement

There is another kind of method which involves a specimen that is smaller than the wavelength. Philippoff and Brodnyan [1955] developed a technique in which the specimen and transmitting liquid were contained within a rigid cylinder in which alternating pressures at 0.0003 to 6 Hz were generated by a mechanically driven piston. After suitable calibrations it was possible to determine K^*, but the friction of variable magnitude between the piston and cylinder caused considerable uncertainties in the determination of the loss modulus K''.

The pressure chamber used in this thesis is based on a device developed by McKinney and Belcher [1959]. The chamber, which consists of two nearly symmetrical pieces bolted together. Within a cylindrical cavity having dimensions small compared to the wavelength at the frequencies employed, are two piezoelectric volume expander transducers mounted on thin copper wires, together with a transmitting fluid and the polymer specimen. One of the transducers is driven by an AC voltage; the other one acts as a pressure sensor to measure the voltage and phase difference relative to the voltage applied to the first transducer. The two transducers are mechanically coupled by the sum of the compliances of the specimen, the transmitting

liquid, the transducers, and the cavity itself.

The relation between the driving (E_1) and output (E_2) voltages is given in terms of the piezoelectric constants of the transducers and the sum of the various compliances by:

$$\left(\frac{E_1}{E_2}\right)^* = C^* + D^*(M_s^* - M_t^*)V_s, \tag{1.36}$$

where M_t^* is the compressibility of the transmitting medium, M_s^* that of the sample. C^* and D^* are complex constants, which are determined by calibrations at each temperature, static pressure, and frequency, using samples of known compressibility.

Chapter 2 Experimental Preliminaries

Among the several means reviewed in the previous chapter that could be useful for the determination of viscoelastic bulk response, the method of determining the dynamic compliance with the aid of piezoelectric volume sensitive drivers and sensors appeared the most reliable. This chapter includes the principle of measurement, the design and operation of the apparatus.

2.1 Principle of Measurement

The method provides a direct measure of volume change with time under sinusoidally varying pressure during a deformation of the sample which involves a change of volume only. [McKinney and Belcher, 1959]

The size of the cavity is much smaller than the wavelength at the frequency range of interest. Thus the force transmitted to the sample is essentially a hydrostatic pressure. Under these conditions the transducers may be regarded as generating and detecting pure volume deformations. The complex compliances of the transducer, of the cavity, of the confining liquid, and of the sample are additive.

For piezoelectric transducers, the relationship between the voltage E and current I, pressure p and rate of volume change $\dot{v}$, can be written as [Trent, 1948]:

$$\begin{bmatrix} E \\ I \end{bmatrix} = \begin{bmatrix} a & b \\ c & d \end{bmatrix} \begin{bmatrix} p \\ \dot{v} \end{bmatrix}, \tag{2.1}$$

where a, b, c and d are complex properties of the piezoelectric transducer. In general, these vary with frequency and temperature.

The reciprocal equation of (2.1) is

$$\begin{bmatrix} p \\ \dot{v} \end{bmatrix} = \begin{bmatrix} e & f \\ g & h \end{bmatrix} \begin{bmatrix} E \\ I \end{bmatrix}, \tag{2.2}$$

where e, f, g and h are "inverses" of a, b, c and d.

A subscript "1" will refer to the driving (input) transducer, "2" to the pickup (output) transducer. Only pressures and volume changes are considered and shearing motions or forces are absent in the discussion. Consequently, the properties of the medium in which the transducers operate can be expressed by

$$\begin{bmatrix} p_i \\ \dot{v}_i \end{bmatrix} = \begin{bmatrix} 1 & 0 \\ i\omega C_a^* & -1 \end{bmatrix} \begin{bmatrix} p_o \\ \dot{v}_o \end{bmatrix}, \tag{2.3}$$

where p_i, $\dot{v}_i$ are the input pressure and rate of volume change (those associated with the medium adjacent to the driving transducer), p_o, $\dot{v}_o$ the output quantities (those associated with the medium adjacent to the pickup crystal), and C_a^* is an acoustic compliance equal to the sum of the compliances of the cavity, the transmitting medium, and the sample.

Because the dimensions of the cavity are such that the pressure at any instant can be considered to be uniform, $p_1 = p_i = p_o = p_2$, which leads to the first part of equation (2.3). The second part in equation (2.3) is derived based on the fact that the total volume change of the medium, the cavity and the sample equals the total compliance times the uniform pressure in the cavity.

$$\dot{v}_i + \dot{v}_o = C_a^* \dot{p}_o = i\omega C_a^* p_o. \tag{2.4}$$

The relation between the currents and voltages of the driving and pickup crystals is

$$\begin{bmatrix} E_1 \\ I_1 \end{bmatrix} = \begin{bmatrix} a_1 & b_1 \\ c_1 & d_1 \end{bmatrix} \begin{bmatrix} 1 & 0 \\ i\omega C_a^* & -1 \end{bmatrix} \begin{bmatrix} e_2 & f_2 \\ g_2 & h_2 \end{bmatrix} \begin{bmatrix} E_2 \\ I_2 \end{bmatrix}. \tag{2.5}$$

Thus

$$\begin{bmatrix} E_1 \\ I_1 \end{bmatrix} = \begin{bmatrix} [e_2(a_1 + b_1 i\omega C_a^*) - b_1 g_2]\, E_2 + [f_2(a_1 + b_1 i\omega C_a^*) - b_1 h_2]\, I_2 \\ [e_2(c_1 + d_1 i\omega C_a^*) - d_1 g_2]\, E_2 + [f_2(c_1 + d_1 i\omega C_a^*) - d_1 h_2]\, I_2 \end{bmatrix}. \tag{2.6}$$

In particular, if I_2 is held equal to be zero (open circuit on the pickup transducer), the ratio of the input to the output voltage is

$$\left(\frac{E_1}{E_2}\right)^* = b_1 e_2 \left[\frac{a_1}{b_1} - \frac{g_2}{e_2} + i\omega C_a^*\right]. \tag{2.7}$$

If the cavity of volume V contains a sample of volume V_s with a compliance M_s and a volume $V - V_s$ of oil having compliance M_t, the total compliance of the cavity, oil, and specimen can be expressed as

$$C_a^* = M_t^*(V - V_s) + M_s^* V_s + C_o^*, \tag{2.8}$$

where C_o^* is the bulk compliance of the transducers, wires, etc. excluding those of the transmitting fluid and specimen.

Substituting (2.8) into equation (2.7) reduces to

$$\left(\frac{E_1}{E_2}\right)^* = C^* + D^*(M_s^* - M_t^*)V_s, \tag{2.9}$$

where

$$C^* = i\omega b_1 e_2, \qquad D^* = b_1 e_2 \left[\frac{a_1}{b_1} - \frac{g_2}{e_2} + i\omega C_o^*\right]$$

are device constants which are not changed by introducing a specimen. No assumptions have been made here as to the values of the crystal constants with respect to frequency, temperature, or static pressure.

The basic assumption in the above derivation is the bilateral relation between the mechanical quantities p, $\dot{v}$ and the electrical quantities E, I during the energy transformation from electrical energy to mechanical energy, or vice versa.

A derivation based on mechanical models is presented here to illustrate the mechanics of the measurement. Since only volumetric deformation is involved in the experiment, the problem can be treated as one-dimensional.

Assuming the size of the cavity is much smaller than the wavelength of the transmitted wave, the pressure is considered uniform in the whole system and the volume

change is governed by

$$\Delta V_1 + \Delta V_2 + \Delta V_3 + \Delta V_4 = 0, \tag{2.10}$$

where ΔV_1 is the volume change on the driving transducer if there is no surrounding constraint applied, ΔV_2 the volume of change of the transmitting oil, ΔV_3 the volume of change of specimen, ΔV_4 the volume change on the pickup transducer.

Thus,

$$\begin{aligned} \Delta V_1 &= -(\Delta V_2 + \Delta V_3 + \Delta V_4) \\ &= -\left[M_t(V - V_s) + M_s^* V_s + C_o^*\right] p, \end{aligned} \tag{2.11}$$

where V is the volume of the cavity (the maximum volume of oil can be filled), M_t and M_s^* the bulk compliance of the transmitting fluid and specimen, V_s is the volume of the specimen. C_o^* includes the sum of all rest of the compliances including cavity wall, wires, transducers, etc.

For the driving piezoelectric transducer as a volume expander, one has, if the surrounding compliance is zero (free spring),

$$\Delta V_1 = \kappa_1 E_1. \tag{2.12}$$

The pickup transducer is a pressure sensor, for which

$$E_2 = \chi_2 p. \tag{2.13}$$

Substituting (2.12) and (2.13) into equation (2.11), one finds

$$\kappa_1 E_1 = -\left[M_t(V - V_s) + M_s^* V_s + C_o^*\right] E_2/\chi_2. \tag{2.14}$$

Therefore,

$$\left(\frac{E_1}{E_2}\right)^* = \frac{M_t(V - V_s) + M_s^* V_s + C_o^*}{\kappa_1 \chi_2}$$
$$= C^* + D^*(M_s^* - M_t)V_s, \qquad (2.15)$$

where

$$C^* = \frac{M_t V + C_o^*}{\kappa_1 \chi_2}, \qquad D^* = \frac{1}{\kappa_1 \chi_2}.$$

Again, C^* and D^* are cavity constants to be determined by calibration. Equation (2.15) is the same as equation (2.9) which was derived by different means.

2.2 Pressure Chamber

The pressure chamber, shown in figure 2.1 and 2.2, is constructed in two cylindrical halves of 303 stainless steel. The initial part of the apparatus was designed by C. Schultheisz. The nearly identical top and bottom are each 12.7 *cm* in outer diameter and 4.5 *cm* high. The mating surfaces are lapped and polished to ensure tight closure of the pressure chamber when the two halves are connected by six bolts (3/8" Allen screws). Needle valves are used in the inlet and outlet oil lines to minimize pressure variations generated in the chamber upon valve closure. Valves and oil fittings were purchased from High Pressure Equipment Company, Erie, PA.

Once the specimen is placed inside the "lower" section of the chamber, the two halves are bolted together. Oil is pumped into the evacuated chamber[1] with a hand pump, until it exits through the top valve. The top valve (outlet) is closed first and the chamber is charged to the desired static pressure, then the bottom valve (inlet) is closed to isolate the chamber (pressure) from the supply and the environment. Prior to charging the hand pump the pressure transmitting oil is de-gassed in a vacuum chamber until no bubbles can be detected. After a container of oil is placed in a vacuum chamber, it is observed that bubbles rises from the bottom or the side

[1]Evacuation before and during the oil-filling procedure to eliminate trapped air in the chamber.

walls of the container. The bubbles get smaller and rise slower during the degassing process. This oil degassing process requires about 24 hours for a liter of oil. To furthur eliminate the existance of air bubbles in transmitting fluid and increase the repeatability of experiment, the specimen and oil are applied to a pressure of 2,000 psi for 1-2 hours before each test. This procedure helps oil to absorb air bubbles. It is estimated an air bubble with diameter of $200\mu m$ can be completely absorbed by oil in an hour.

The cavity detail is sketched in figure 2.3. The cylindrical cavity is 0.9 *cm* high by 1.0 *cm* in diameter. A copper mesh mounted in the bottom half of the pressure chamber supports the specimen. The chamber is sealed by means of a Sirracin-Harrison K-Seal which can be used with temperatures as high as 315°C and pressures of up to 410 MPa (70,000 psi).[2] Copper washers are used jointly with the K-Seal to obtain more consistent oil sealing. New copper washers are used each time the chamber is closed, so that a K-seal can be used repeatedly.[3] Since the sealing reliability depends on placing the components in nearly identical position relative to each other, alignment pins are used between the two chamber halves.

2.3 Piezoelectric Transducers and Electrical Feed-through

The piezoelectric transducers are identical Lead Metaniobate disks 1.0 *mm* thick and 7.5 *mm* in diameter, which are usable to temperatures of 300°C and at pressures of up to 70 MPa. The transducers were purchased from Piezo Kinetics Inc., Bellefonte, PA. The relevant properties for the Lead Metaniobate piezoelectric disks are listed below,

[2]At this time no measurements at elevated pressures have been made, though they are intended later. Also, the apparatus has been designed to accommodate materials with higher glass transition temperatures.

[3]Each compression of the K-seal causes a tiny compression set; this cumulative effect is alleviated through the use of fresh copper washers.

Physical Properties	
Density	6 $gram/cm^2$
Curie Temperature	450°C
Mechanical Q	15 Maximum
Resonant Frequency	137,000 Hz
Dielectric Properties	
Dielectric Constants	275 ± 10%
Dissipation Factor	1% Maximum
Resistivity	$10^{12}\Omega$
Piezoelectric Properties	
Coupling Coefficients	
k_{33}	0.35
d_{33}	$80 \times 10^{12} m/V$
k_{33}	$33 \times 10^{3} m/N$

The flat surfaces of the transducer disks are silver coated for solder connections of copper leads. One face of each transducer disk is grounded to the pressure chamber through a mechanical pin connection while the other face is connected to respective electrodes via thin spiral copper wires.

An important detail in the operation is a trouble free electrical communication from the cavity to the measuring circuit. For working with elevated pressures the electrical connections must be passed pressure-tight through the cavity walls. Electrical connections[4] are made by passing the electrodes through the small holes (1.78 mm in diameter) in both halves of the pressure chamber. The assembly of the electrode is shown in figure 2.5. The screw plugs function as both electrodes and sealing plugs for transmitting oil. The oil sealing and electricity insulation are achieved by using thin Teflon washers. The screws have to be tightened with sufficient force to form the

[4]Shielded BNC connectors and shielded cables are essential to reduce noise on both piezoelectric transducers.

oil seal but not too tightly so as not to damage the electrical insulation. High temperature epoxy adhesives were tried in the electrical connection but were unreliable because their coefficients of thermal expansion are substantially different from that of steel.

2.4 Measurement Circuitry

The schematic of the circuit for measuring the output of the piezoelectric disk is shown in figure 2.6. It consists of an SRS lock-in amplifier, a charge amplifier, and a digital oscilloscope as monitor.

2.4.1 Lock-in Amplifier

A Stanford Research Systems (SRS) dual phase digital lock-in amplifier (Model DSP SR830) and a charge amplifier are used to measure the voltage on the output piezoelectric transducer. The lock-in amplifier is capable of measuring the in-phase and out-of-phase signal relative to the reference signal with an accuracy of 0.001 mV.

A lock-in amplifier has the ability to measure the signal in a very narrow frequency band-width so that it targets the signal measurement at a specific frequency. Lock-in amplifiers use a technique known as phase-sensitive detection (PSD) to single out the component of the signal at a specific reference frequency and phase. Noise signals at frequencies other than the reference frequency are rejected and do not affect the measurement. The phase sensitive detection is able to sense the signal with a bandwidth as narrow as 0.01 Hz. The lock-in amplifier requires a frequency reference, which in the current experiment is just the input frequency on the driving piezoelectric transducer.

A function generator built into the SRS SR830 lock-in amplifier produces the sinusoidal voltage (5V maximum) fed to the piezoelectric disk which serves as a volume expander. The reference frequency of the lock-in amplifier is set internally to the frequency of the signal generated by the function generator. In this way the noise level is reduced dramatically because the amplifier responds only to the frequency

of the signal applied to the input transducer. Besides the high resolution of the lock-in amplifier its important contribution to the precision of the measurements is thus that they can all be made at very precisely predetermined frequencies and that interpolation between multiple measurements (calibration, see below) is obviated. The frequency as controlled by a digital SRS SR830 lock-in amplifier is accurate to 0.1 mHz. A digital oscilloscope (Nicolet Model 4049) monitors the output signal from the pickup transducer through the lock-in amplifier.

2.4.2 Piezoelectric Charge Amplifier

A piezoelectric transducer charge amplifier was built using a Bur-Brown OPA128 operational amplifier (c.f. figure 2.8) to possess a low cut-off frequency of 0.16 Hz. The OPA128 has excellent low-level signal handling capability and has a differential impedance of $10^{13}\Omega$. Because of this very high impedance, it becomes, however, the source of many kinds of noise, principally via electro-magnetic interference from the input wires of the amplifier. All leads must thus be carefully shielded and grounded to reduce the noise level. The output from the pick-up piezoelectric transducer is less than 5 mV (RMS) for a 5V (RMS) input to the driving transducer. Achieving a high electronic signal/noise ratio is, therefore, essential to obtain accurate bulk compliance measurements.

2.5 Thermal Control

The pressure cell is housed in a Grieve HT-800 industrial oven operating on a Honeywell (model UDC 3000) temperature controller. The temperature of the pressure chamber is monitored by nickel-iron thermocouples and temperature control is accurate to 0.1°C. The thermocouple leads are passed through the oil outlet to be as close to the cavity as possible; this thermocouple is withdrawn once the final temperature is reached and before measurements commenced. Because of the large thermal mass of the pressure cell typically three to four hours are required for the temperature to stabilize in the cavity. In order to prevent thermal pressure built up in the cavity,

inlet and outlet oil ports are left open until the temperature has stabilized after which the valves are closed and another 1-2 hours passes before any measurements are made. Once the desired temperature has been reached, it remains very constant because of the large thermal mass. Nevertheless, a time span of one to two hours is allowed to pass after withdrawal of the thermocouple in order to assure complete temperature stabilization.

2.6 The Frequency Range and Automation of the Experiment

There are two limitations to the useful frequency range: The upper frequency limit is governed by the size of the pressure cavity in that the dimensions of the specimen and of the cavity have to be small compared to the length of the pressure wave in the transmitting fluid; the lowest resonance frequency is around 10 kHz.

The resonance is caused by the standing waves inside of the cavity and possibly by the wave reflection on the walls of the pressure chamber.

Figure 2.10 shows the response of the apparatus over a large frequency range in which the response is most near to constant values in the range from 10 to 1,000 Hz, which was the range chosen for the subsequent measurements. The lower frequency limit is imposed by the low frequency response of piezoelectric transducers which makes these devices virtually useless much below one Hz. For future operations expansion to three decades (3 to 3 kHz) is considered.

Under these conditions measurements can be considered as adiabatic. Marvin and McKinney [1965] deduced the "critical" frequency for meeting adiabatic conditions of the sample as $f_c = \kappa/(C_p \rho x^2)$, where f_c is the critical frequency, C_p the specific heat at constant pressure, ρ the density of the sample, x the thickness of the specimen, κ the thermal conductivity of the polymer material. Based on this argument the critical frequency would be on the order of 0.01 Hz. At and above this frequency value there is insufficient time for appreciable heat conduction. Below this frequency measurements tend toward isothermal response.

The experiment is controlled by a computer (IBM 486DX2 66 MHz) through

serial communications with the SRS lock-in amplifier. The input voltage to the driving piezoelectric transducer is 5V which is the maximum output from the built-in function generator. The computer sends out a command to set the frequency of the function generator, then waits for 30 seconds before it starts recording in-phase and out-of-phase voltages from the pick-up transducer. The voltages are sampled 30 times for 30 seconds, then averaged to reduce the random statistical error and stored on a hard disk. This procedure is repeated for each temperature, computer controlled, over the frequency range of the experiment.

2.7 Calibration

Because there are many parameters contributing to the final results which cannot be accounted for on the basis of "first principles" the key to successful measurements is a careful calibration.

The complex constant C^* is just the complex input/output voltage ratio $(\frac{E_1}{E_2})^*$ when the cavity is filled with oil only ($V_s = 0$). In order to determine the constant D^*, differentiate equation (2.9) with respect to V_s,

$$\frac{\partial}{\partial V_s}\left(\frac{E_1}{E_2}\right)^* = D^*(M_s^* - M_t). \tag{2.16}$$

If a sample with known bulk compliance M_s^* is placed in the cavity, the constant D^* can be determined using samples of different sizes from the slope of the $(\frac{E_1}{E_2})^*$ versus V_s lines.

The calibrations of the pressure chamber to determine the two constants C^* and D^* were conducted on an oil-filled cavity (no specimen) and with iron samples over the same range of frequencies and temperatures. Same transmitting fluid is used as McKinney and Belcher (Di-2-ethylhexyl sebacate) so that the oil compressibility from that work is available. The compressibility of the transmitting oil is listed in table 2.1 at different temperatures.

While one would expect purely elastic response of the system with oil and iron in the cavity, the detailed transducer response to sinusoidal excitation is not very well

Temperature($°C$)	Compressibility of the transmitting fluid (1/GPa)
22	0.4732
25	0.4878
30	0.5025
35	0.5173
40	0.5323
45	0.5475
50	0.5628
55	0.5782
60	0.5939
65	0.6097

Table 2.1: Compressibility of transmitting fluid.

understood. The system requires then careful calibration over the whole range of frequency and temperature. The bulk compliance of iron is $0.587 \times 10^{-11} m^2/N$ and independent of temperature in the range of these studies. The volume of the cavity in the pressure chamber is 0.785 cm^3. Four iron samples in the shape of circular disks were used for calibration, as shown in figure 2.12. The volume of the iron pieces are 0.050, 0.074, 0.099, and 0.152 cm^3 respectively.

Figure 2.13 shows the amplitude of the output voltage from the pickup transducer while the input voltage on the driving transducer is held at 5V. Third order polynomial curve segments are fitted to the data to generate the smooth connections between data points. Additional calibration samples #1 (0.050 cm^3) and #2 (0.074 cm^3) were placed in the cavity to form samples of different volume (0.124 cm^3). It is clearly seen from figure 2.13 that the curves for different volumes of iron samples are parallel to each other. The voltage magnitude from the pickup transducer increases as the volume of iron sample increases, because the bulk compliance of iron is smaller than that of the transmitting oil ($M_c - M_t < 0$). Figure 2.14 shows the phase shift angle between input and output signals for the cases with oil only in the cavity, and with different sizes of iron sample introduced. It can be seen that the introduction of iron samples does not change the phase shift. Therefore, the response from transmitting oil is linearly elastic. This same calibration procedure to determine C^* and D^* also

serves to confirm that the compressibility of the transmitting liquid used is real over the frequency range employed.

For calibration purposes, equation (2.9) becomes

$$\left(\frac{E_1}{E_2}\right)^* = C^* + D^*(M_c - M_t)V_c, \tag{2.17}$$

where the subscript "c" indicates calibration. In equation (2.18) only the voltage ratio and two undetermined constants are complex numbers; therefore one can separate the real and imaginary parts easily to determine complex constant D^*.

$$\left(\frac{E_1}{E_2}\right)_{in-phase} = Re(C^*) + Re(D^*)[M_c - M_t]V_c, \tag{2.18}$$

$$\left(\frac{E_1}{E_2}\right)_{out-of-phase} = Im(C^*) + Im(D^*)[M_c - M_t]V_c. \tag{2.19}$$

Figure 2.15 shows the in-phase and out-of-phase voltage from output transducer as a function of iron sample volume at frequencies of 10, 100 and 1000 Hz. The slopes of the lines determine the real and imaginary parts of D^*, which are displayed in figure 2.16 in the frequency range from 1 to 1,000 Hz.

2.8 Calculation of the Bulk Compliance

In the transducer equation (2.9) it is required that the volume of the sample be known as a function of temperature in order to calculate its dynamic bulk compliance. The specific volume of PVAc was determined by Heymans [1983] using a glass dilatometer with mercury as a confining liquid.

The specific volume of PVAc as a function of temperature is shown in figure 2.17. The values of specific volume at temperatures of measurements are listed in table 2.2. The glass transition temperature of PVAc determined from the graph of specific volume is 29.5°C, which is the transition point for the slope or thermal coefficient of expansion. The values of the cubical thermal coefficient of expansion is $2.50 \times 10^{-4}/°C$ in the glassy domain and $5.98 \times 10^{-4}/°C$ in the rubbery domain.

Temperature (°C)	Specific volume (cm^3/g)
20	0.8402
22	0.8402
25	0.8412
30	0.8431
35	0.8455
40	0.8481
45	0.8508
50	0.8535
55	0.8562
60	0.8588
65	0.8615

Table 2.2: Specific Volume of PVAc

After the constants C^* and D^* are determined from the calibration, the compressibility of the sample is calculated by

$$M_s^* = M_t + \frac{(\frac{E_1}{E_2})_s^* - (\frac{E_1}{E_2})_o^*}{V_s D^*}, \tag{2.20}$$

where $(\frac{E_1}{E_2})_o^*$ is the complex voltage ratio for oil only, while $(\frac{E_1}{E_2})_s^*$ is the complex voltage ratio for the situation where a polymer specimen is in the cavity.

An example of the in-phase and out-of-phase voltages from the output piezoelectric transducer is shown in figure 2.18. The bulk modulus is calculated from the in-phase and out-of-phase voltage ratio using equation (2.21). A computer program written in C for the calculation can be found in Appendix II. Measurements were actually carried out at frequencies from 2 to 5,000 Hz, but because of the poor responses at high and low frequencies only data between 10 and 1,000 Hz were processed.

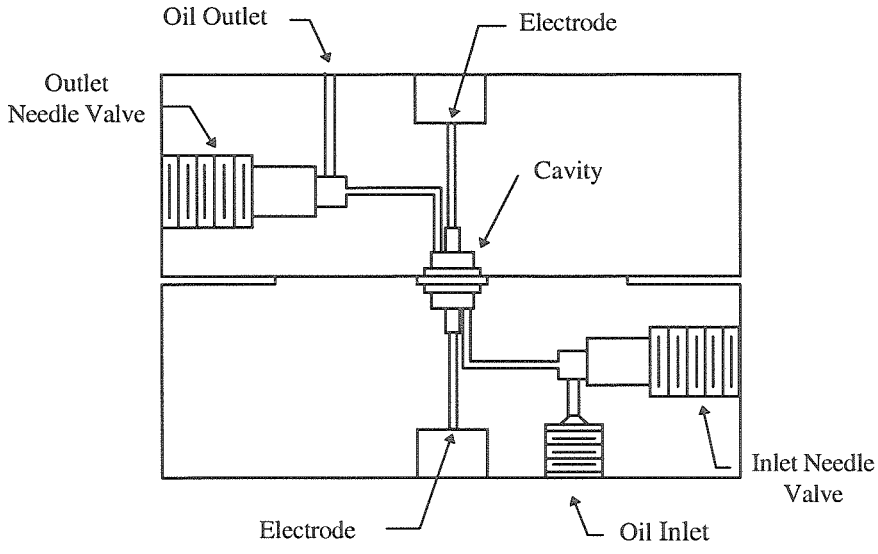

Figure 2.1: Pressure chamber.

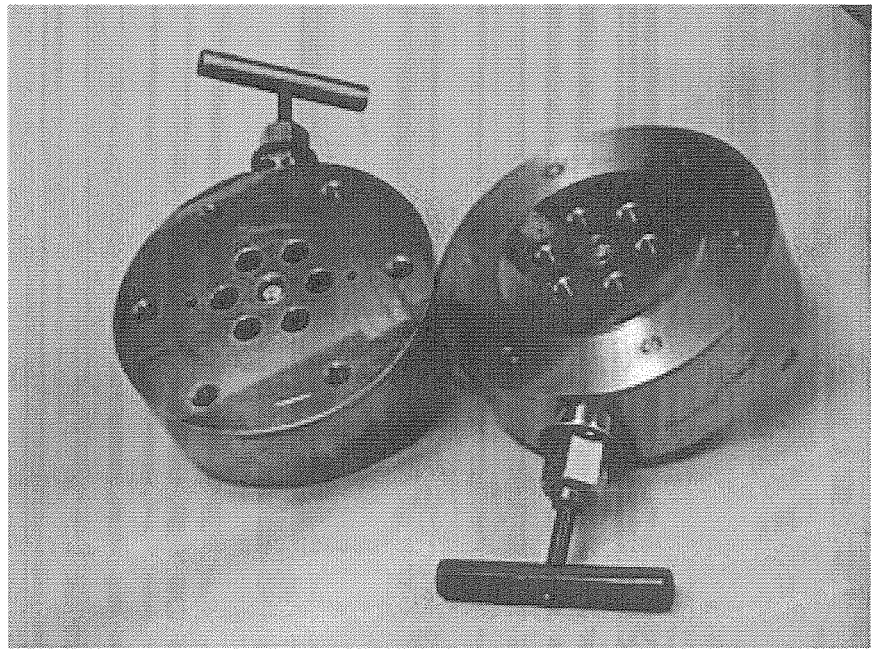

Figure 2.2: Picture of pressure chamber.

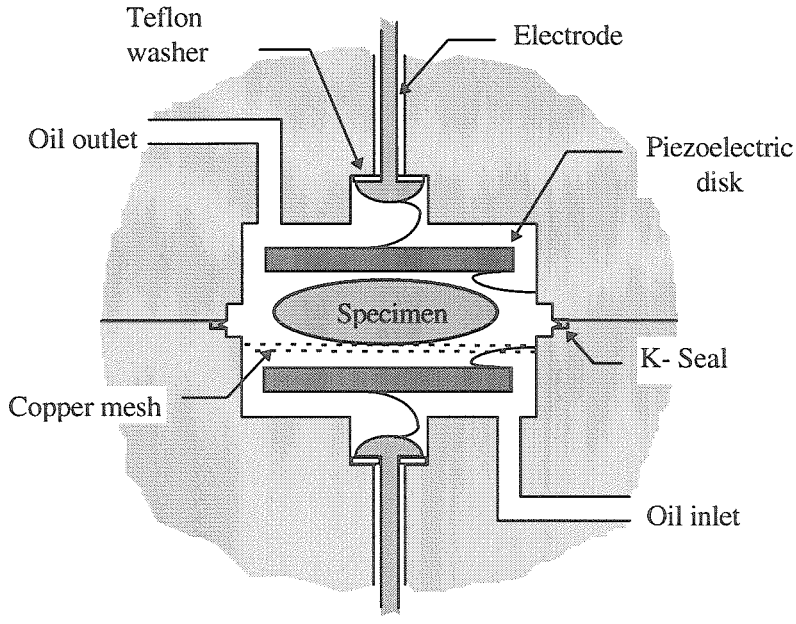

Figure 2.3: Cavity and piezoelectric transducers.

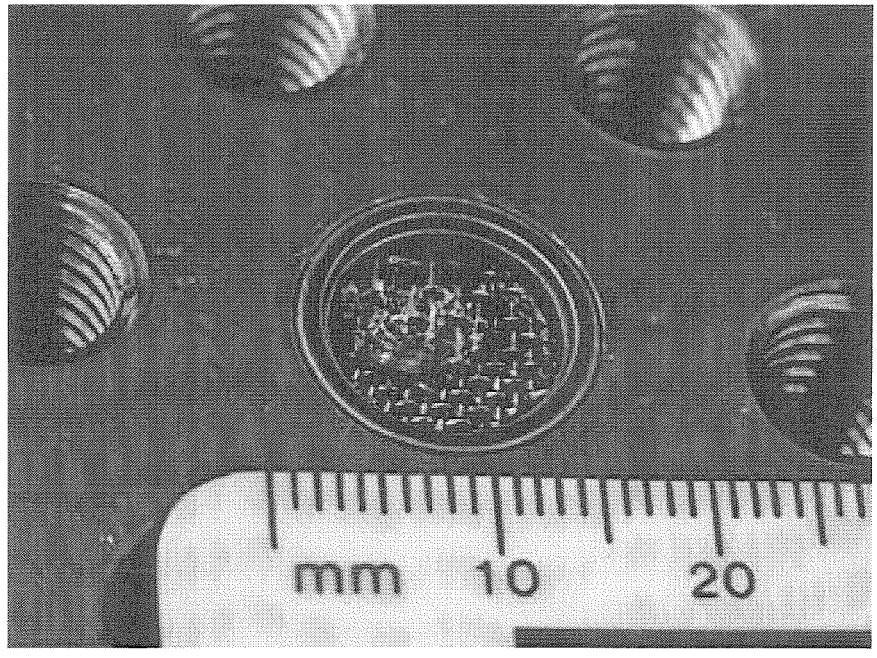

Figure 2.4: Picture of cavity and a PVAc specimen inside.

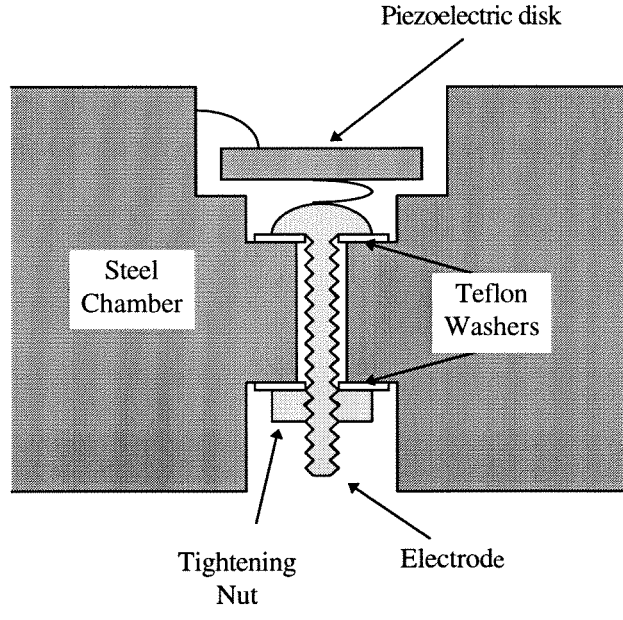

Figure 2.5: Electrode assembly.

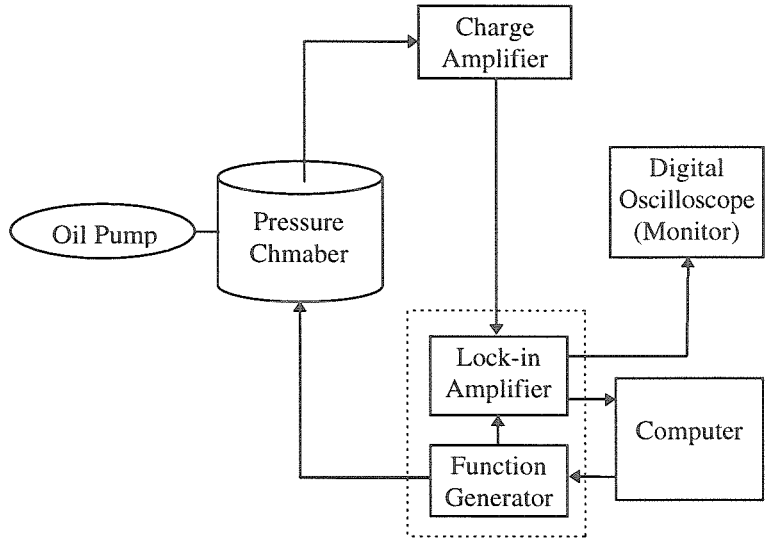

Figure 2.6: Experimental setup.

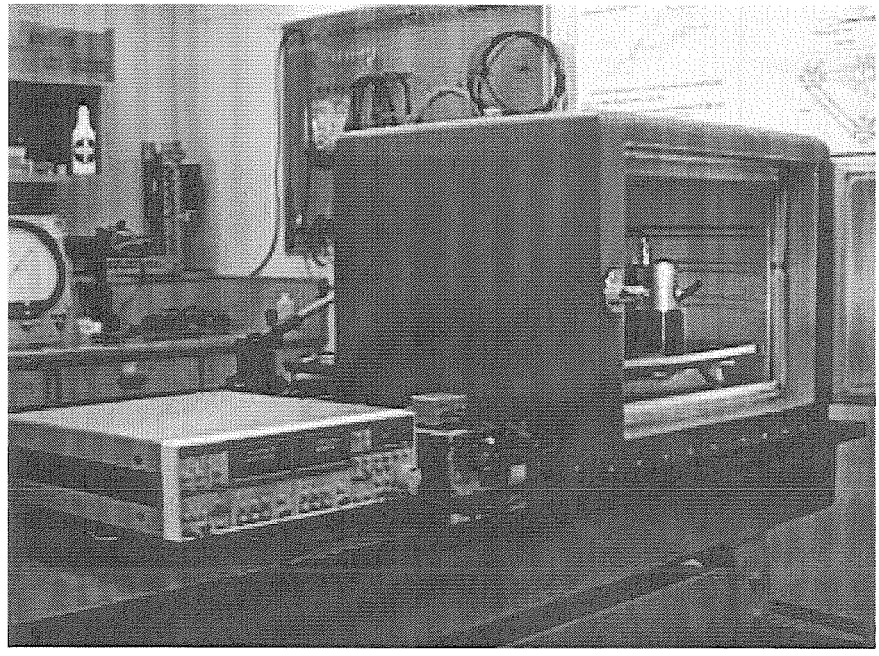

Figure 2.7: Picture of the experimental setup.

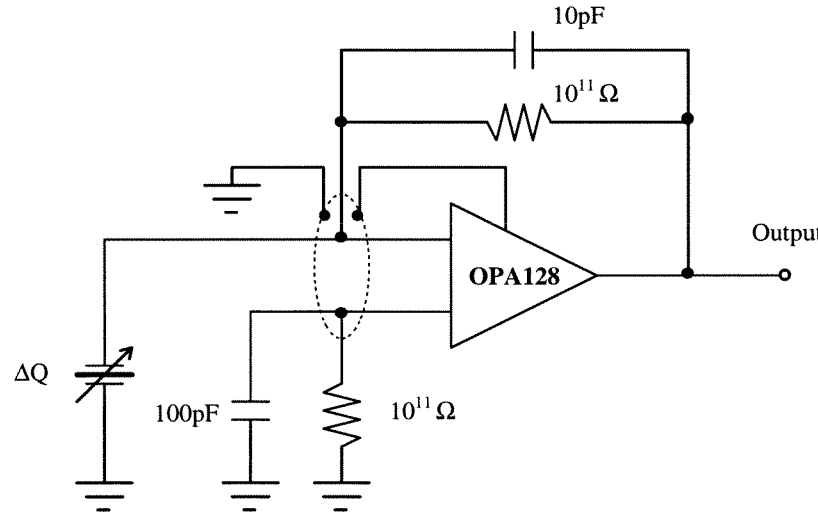

Figure 2.8: Piezoelectric transducer charge amplifier.

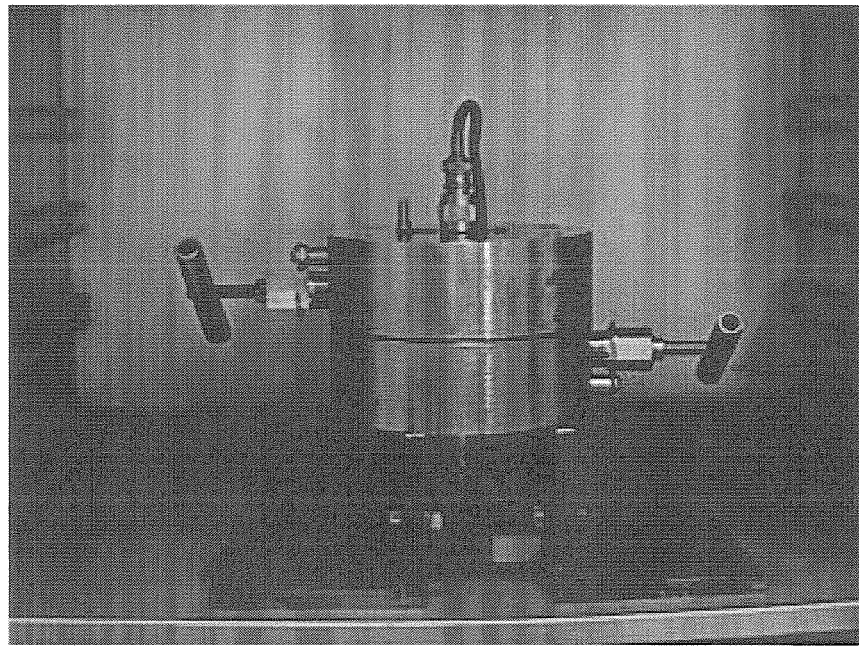

Figure 2.9: Picture of assembled pressure chamber.

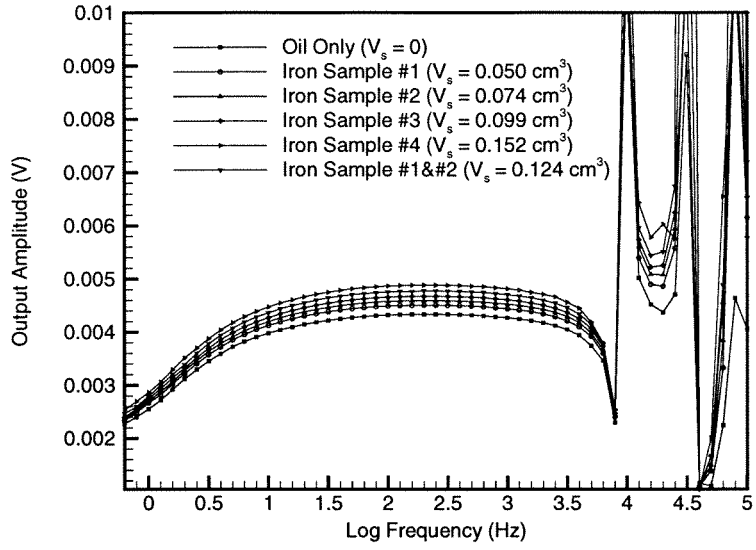

Figure 2.10: Output voltage on the pickup piezoelectric transducer in a wide frequency range.

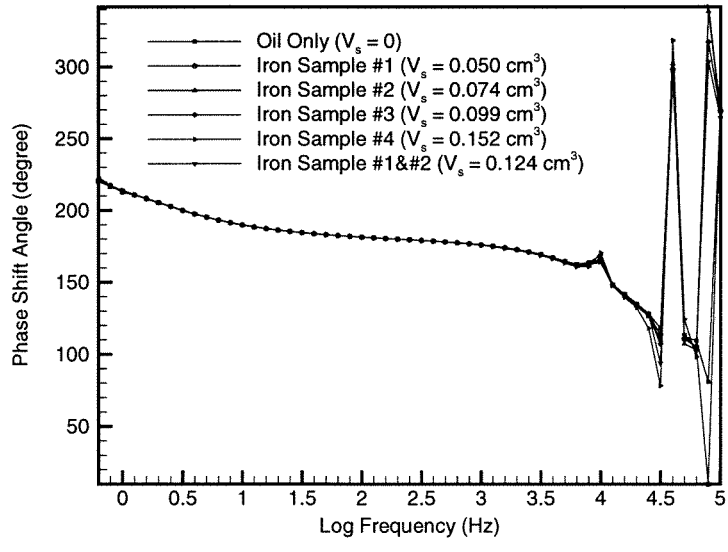

Figure 2.11: Phase shift between input and output voltages in a wide frequency range.

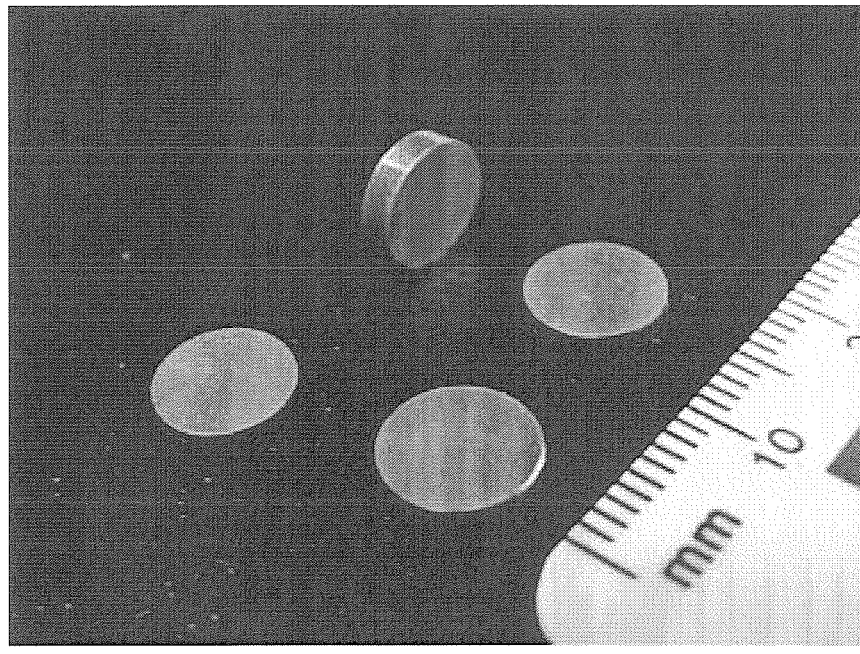

Figure 2.12: Picture of the iron samples for calibration.

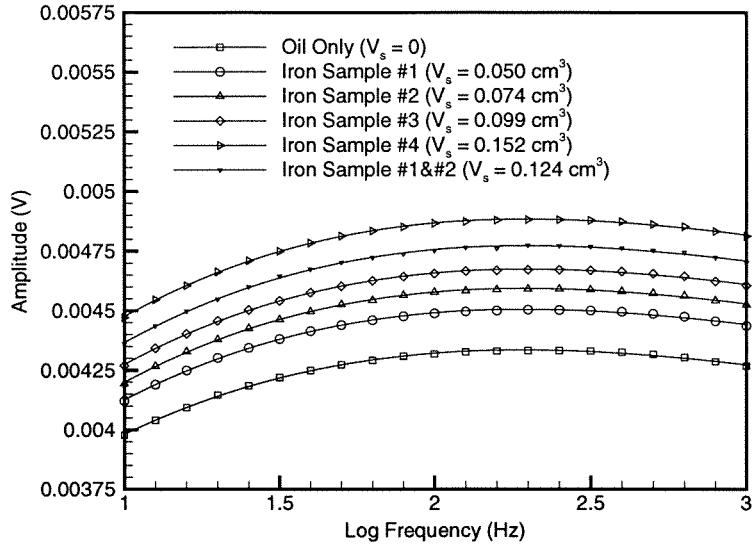

Figure 2.13: Output magnitude for different iron samples.

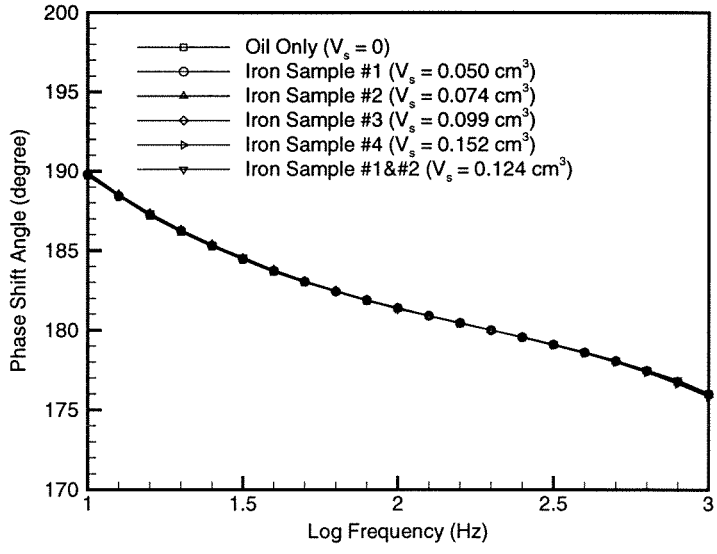

Figure 2.14: Output phase shift for different iron samples.

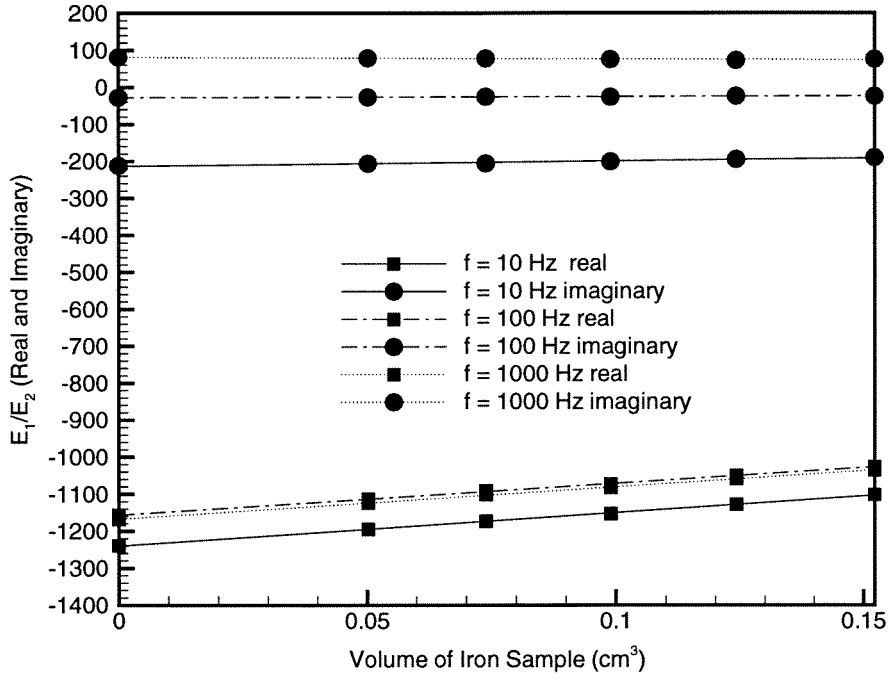

Figure 2.15: Input/output ratio verses volume of iron sample.

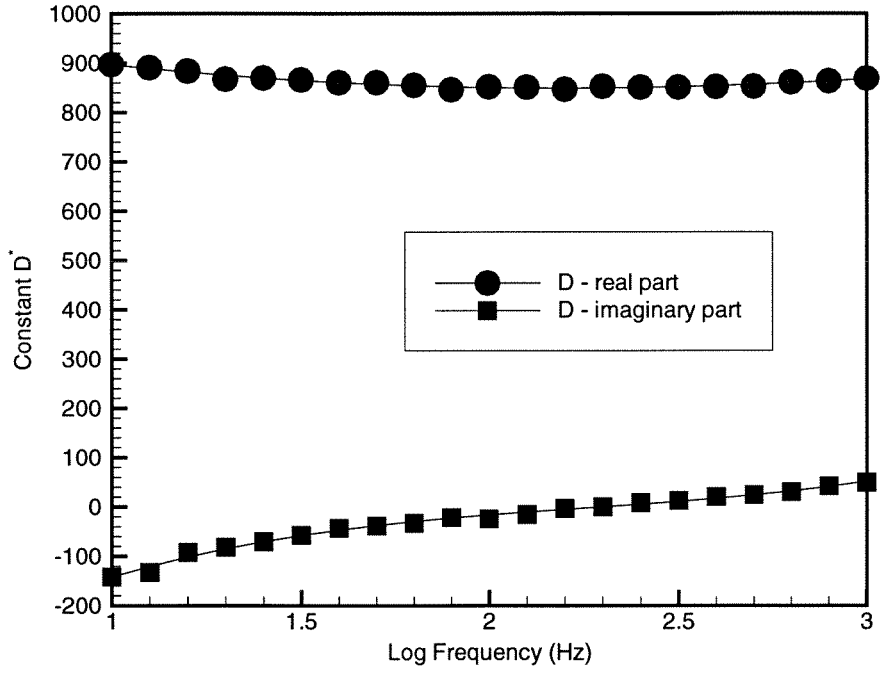

Figure 2.16: Real and imaginary parts of constant D^* at frequencies between 10 to 1000 Hz.

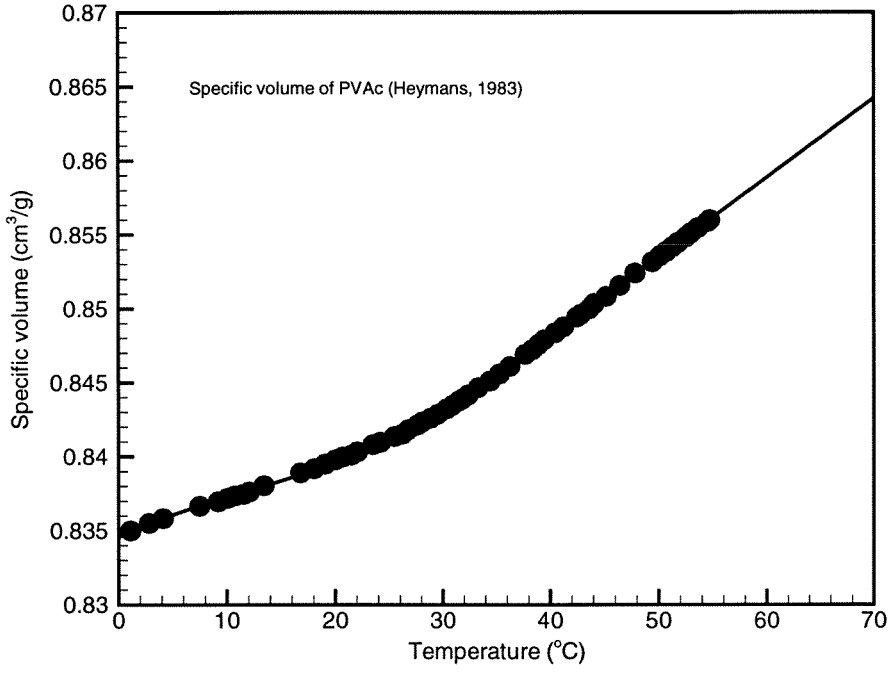

Figure 2.17: Specific volume of PVAc

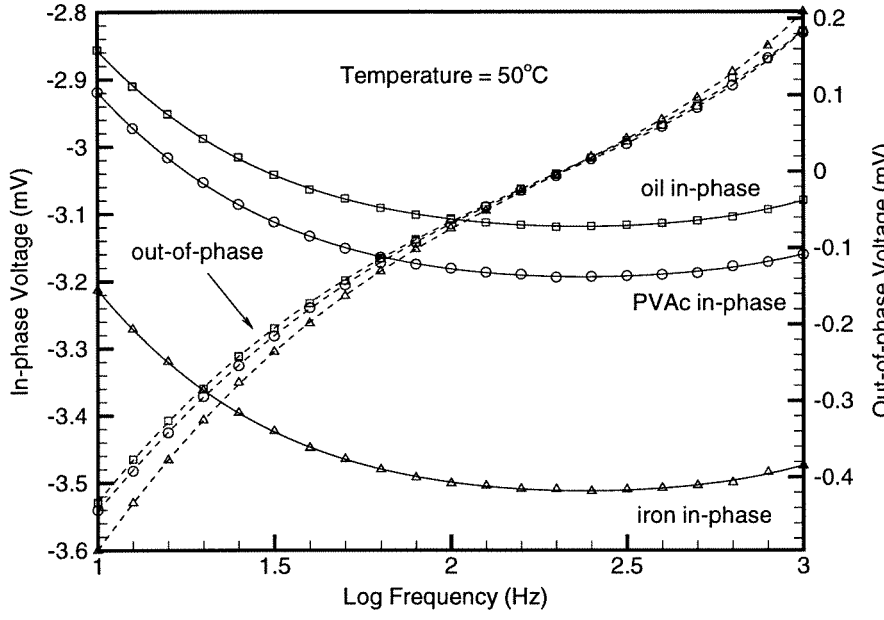

Figure 2.18: Example of in-phase (left ordinate) and out-of-phase (right ordinate) output voltages for oil, iron and PVAc in the cavity at 50°C.

Chapter 3 Results and Discussion

In this chapter the detailed measurements on bulk compliance of poly(vinyl acetate) are presented. The results are discussed and evaluated relative to the bulk and shear response as measured by other investigators.

3.1 Specimen

The PVAc was purchased from Aldrich Chemical Company, and was nominally identical to the material used in earlier studies [Heymans, Emri and Knauss, Kenner and Knauss], with an average molecular weight of 16,700 and a density of 1.191 g/cm^3. The glass transition temperature as quoted by the manufacturer is 30°C which agrees closely with the value of 29.5°C determined by Heymans. The PVAc specimens were in the form of pellets with weight ranging from 0.1 to 0.3 gram. The pellets were kept refrigerated in a sealed container before they were used as specimens in the experiment. Each sample selected was microscopically examined to ascertain that it was void-free. The specimen volume was determined from the weight and the specific volume of PVAc at different temperatures.

The weight of the specimen pellets was checked repeatedly before and after the compliance measurements to detect any swelling or oil absorption. It was found that the weight of the pellets as measured by a Mettler HL32 digital balance with a precision of 1 mg remained constant even after extensive exposure to the oil. The shape of the samples, however, changed during the sequence of measurements because tests were conducted well above the glass transition temperature so that the samples could deform under their own weight.

In a separate test, eight pieces of PVAc pellets were placed into separate containers filled with transmitting oil and weighted by the digital scale on a daily basis, as shown in table 3.1. The Mettler digital scale has a reading of 0.1 mg but the last digit fluctuates by $\pm 0.5mg$, therefore the precision is considered to be on the order

Time(days)	Weight of PVAc specimen(grams)							
0	0.2021	0.1946	0.2229	0.1981	0.2149	0.1808	0.1910	0.2512
1	0.2024	0.1944	0.2229	0.1978	0.2149	0.1806	0.1906	0.2509
2	0.2022	0.1947	0.2231	0.1981	0.2149	0.1805	0.1910	0.2513
3	0.2026	0.1943	0.2230	0.1978	0.2148	0.1805	0.1910	0.2512
5	0.2027	0.1943	0.2230	0.1978	0.2148	0.1807	0.1910	0.2516
8	0.2023	0.1942	0.2228	0.1978	0.2148	0.1807	0.1910	0.2515
13	0.2022	0.1942	0.2227	0.1980	0.2146	0.1809	0.1909	0.2514
20	0.2019	0.1939	0.2222	0.1971	0.2142	0.1803	0.1902	0.2510
28	0.2019	0.1941	0.2224	0.1973	0.2144	0.1807	0.1908	0.2511

Table 3.1: Weight of PVAc samples.

of 1 *mg*. One notices from the table that no weight change is observed within the accuracy of the scale of 1 *mg*. Consider the weight of a PVAc pellet of 0.2 g or 200 mg, one concludes that the weight change due to the oil absorption is less than 0.5% of its weight. Before the pellet was weighed on the scale, it was cleaned by soft paper to remove oil from its surface. No chemical solvent was used in cleaning.

The volumetric strain of the specimen due to piezoelectric transducer volume expansion is on the order of 10^{-6}.

3.2 Piezoelectric Transducer Output

The magnitude ratio and phase shift between input/output voltage at temperature from 22°C to 65°C are shown in figures included in Appendix III. The input voltage on the driving piezoelectric transducer is set to 5V, while the output voltage from the pickup transducer is on the order of millivolts. The dependence of the output voltage on frequency can be seen from these figures and that the magnitude of the output is lower at both low (10 Hz) and high (1000 Hz) frequencies. The curves of magnitude for the cavity filled with oil only and oil plus iron sample fall into a similar pattern, but shifted vertically. There is basically no difference in the phase shift between the case of oil and iron. In the figures of magnitude ratio, the PVAc curve is between those of oil and iron, which means the bulk compliance of PVAc is between that of the

transmitting oil and iron. As the temperature increases, the curve for PVAc moves closer to the curve for the transmitting oil. The phase shifts of PVAc deviate from that of oil and iron, which is obvious at temperatures of 30, 35 and 40°C. (cf figures 4.6, 4.8, 4.10) At the lower temperature of 25°C, it is observed that the phase shift is the same for three cases at high frequency range (close to 1000 Hz) while the value of phase shift is higher at the lower frequency range (close to 10 Hz). The maximum phase shift difference detected was about 0.2 degree, which required high accuracy of the electronic equipment for the measurement at this low signal level.

The temperature dependence of the voltage from the output transducer is shown in figures 3.1, 3.2 and 3.3. The in-phase and out-of-phase output voltages are shown in these figures at temperatures from 25 to 65°C. For each case, oil only, iron sample and PVAc specimen, the magnitude decreases with an increase in the temperature. The phase shift also changes with temperature. Therefore, precise control and measurement of the temperature is important in the experiment to obtain accurate measurements of the bulk compliance because the test requires repeated runs at the same conditions on temperature, static pressure, magnitude and frequency of the input voltage.

3.3 The Bulk Compliance of PVAc

The storage and loss bulk compliances of PVAc at different temperatures and at the frequencies from 10 to 1,000 Hz are displayed individually in figures 3.4 to 3.13, and summarized in 3.14 The most pronounced change in the frequency dependent bulk compliance occurs at temperatures from 30 to 40°C. At a lower temperatures (proximate bulk glassy state)[1] or higher temperatures (near-rubbery bulk state), the bulk compliance remains rather constant.

The data in figure 3.14 are shown shifted in figure 3.15 according to time-temperature superposition to produce a master curve. Rubber elasticity and thermal expansion

[1]The temperature control chamber did not allow for reliable temperature control below room temperature. Thus the lowest temperature recorded is 22°C. Low temperature measurements are currently conducted in a different temperature chamber.

corrections were both applied in the shifting to form the master curve of bulk compliance. The same shift factor is used for storage and loss bulk compliance shift along the log frequency axis. The corresponding shift factors are shown in figure 3.16. The storage and loss compliances are not independent, so that the loss part can be computed from the storage modulus [Ferry, 1980].

$$M' = M_g + \frac{2}{\pi}\int_{-\infty}^{\infty}[M''(\omega)\omega^2/(\omega^2-\omega_1^2)]d\ln\omega, \tag{3.1}$$

$$M'' = \frac{2}{\pi}\int_{-\infty}^{\infty}[(M'(\omega)-M_g)\omega_1\omega/(\omega_1^2-\omega^2)]d\ln\omega. \tag{3.2}$$

To calculate M'' from M', it is necessary to evaluate the integral numerically for each desired frequency ω_1. The integrand has a singularity at $\omega=\omega_1$ (shown in figure 3.17) and the principal value of the integrand is evaluated at ω_1.

Inasmuch as the loss compliance is so small and thus more subject to measurement errors, it is appropriate to examine its consistency in magnitude and frequency dependence with the storage modulus. Accordingly, the curve "A" fitted to the storage compliance in figure 3.15, is used to determine (numerically) the corresponding loss compliance, which is then shown as curve "B" in the same figure. It is seen that the agreement is very satisfactory.

The dynamic bulk modulus of PVAc at 40°C is calculated using equations (1.22) and (1.23) and is shown in figure 3.18.

3.4 Comparison with Other PVAc Data

Having determined the bulk compliance over a significant time or frequency range it is of interest to compare this information with other data on PVAc, notably with the bulk data of McKinney and Belcher [1963], but also with time dependent shear behavior on the same material such as offered by Knauss and Kenner [1980], Heymans [1983], and Plazek [1980]. Figure 3.19 shows the master curves for the storage and loss compliance of the McKinney and Belcher material along with the present data. While

the bulk measurements agree in the bulk rubbery domain, they differ in magnitude across the transition range, yielding a glassy-to-rubbery modulus ratio of about 1.9 for the present data as compared with a corresponding value of 1.6 for the McKinney and Belcher data.[2] In addition, the transition of the present data spans a larger frequency range, being in excess of ten decades as compared to a range of about half that size for the McKinney and Belcher results.

It has often been argued that the transition of the bulk response should be shorter than that of the shear behavior, because the number of molecular deformation mechanisms contributing to bulk deformations should be markedly smaller than those that control shear behavior. With this idea in mind we show in figure 3.20 the dynamic shear compliance for the same Aldrich material used in the bulk deformation studies as computed from Knauss and Kenner's data [1980] together with Heymans' [1983] and Plazek's [1980] results. We note that the transition ranges for the shear and for the bulk responses are comparable, seemingly contradicting the idea that bulk deformation involves fewer relaxation times than shear response.

More important, however, is the fact that the transition ranges for the two material functions do not overlap materially: The bulk response exhibits its transitions behavior in essentially the glassy (high frequency) domain of the shear behavior, with the two transition ranges being separated by about ten to twelve decades. This significant difference in the mean time of the transition ranges of the two material functions indicates that the molecular contributions to these two types of deformations mechanisms derive from different chain and/or side-group mobilities. For shear deformation the molecular chains of polymer require long range movement to adjust to the shape change of a polymer body. The relative movement between molecular chains, for example, sliding, entanglement and rotation of side branches all contribute to the viscoelastic behavior. On the other hand, bulk deformation mainly involves relatively local movement of molecules. The local displacement does cause viscoelastic behavior on the bulk property of polymers, but it is much less significant compared

[2]The corresponding range for medium molecular weight PVAc as measured by Lin and Nolle [1989] appears to be about 2.6.

with shear modulus. The relaxation time for the bulk modulus is also much smaller than shear modulus because local movement of chain-like molecules needs less time than the long-range movement of molecules from each other. This observation for the (very) small deformation (strain on the order of 10^{-6}) behavior (linearly viscoelastic range) is at variance with the response at moderate but non-infinitesimal deformations for which there exists a distinct interaction between shear and dilatational stress and deformation states in determining the time dependent material response [Lu and Knauss,1996].

The difference in molecular deformation sources is also apparent in the comparison of the shift-factors as derived from the bulk data with those obtained from the shear data. In figure 3.16 the solid data points represent the shift factors derived in forming the bulk compliance master curves in figure 3.15, while the open symbols represent the shift data derived in producing the shear modulus data in figure 3.20. Inasmuch as the temperatures are principally above the glass transition the WLF response appears appropriate for the shear data. On the other hand, the bulk response elicits a shift behavior that is much more akin to Arrhenius behavior with a more linear relation than the WLF equation would represent.

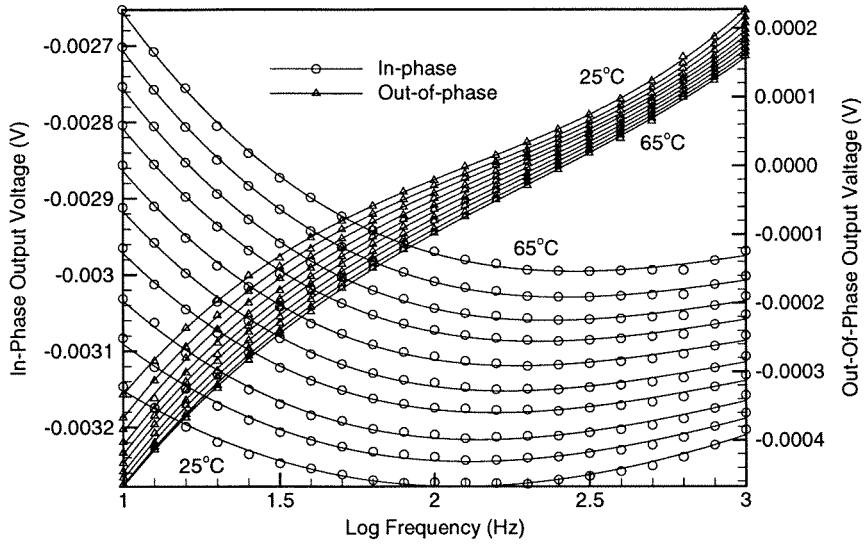

Figure 3.1: In-phase and out-of-phase voltage output with oil only in the cavity, temperature ranges from 25 to 65°C in 5°C intervals.

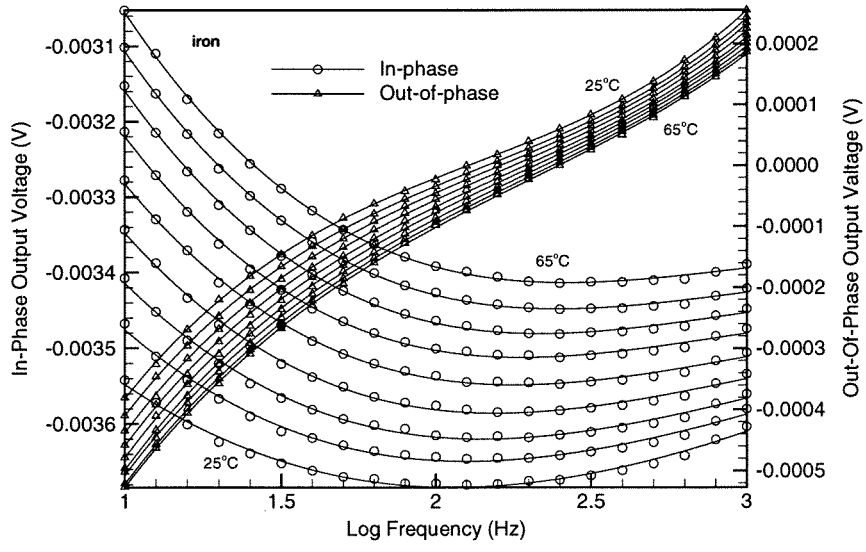

Figure 3.2: In-phase and out-of-phase voltage output with iron sample in the cavity, temperature ranges from 25 to 65°C in 5°C intervals.

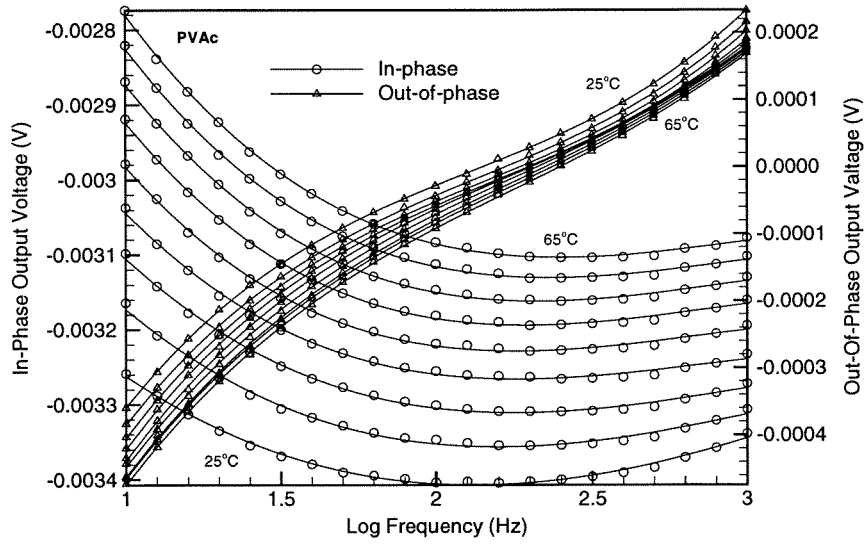

Figure 3.3: In-phase and out-of-phase voltage output with PVAc specimen in the cavity, temperature ranges from 25 to 65°C in 5°C intervals.

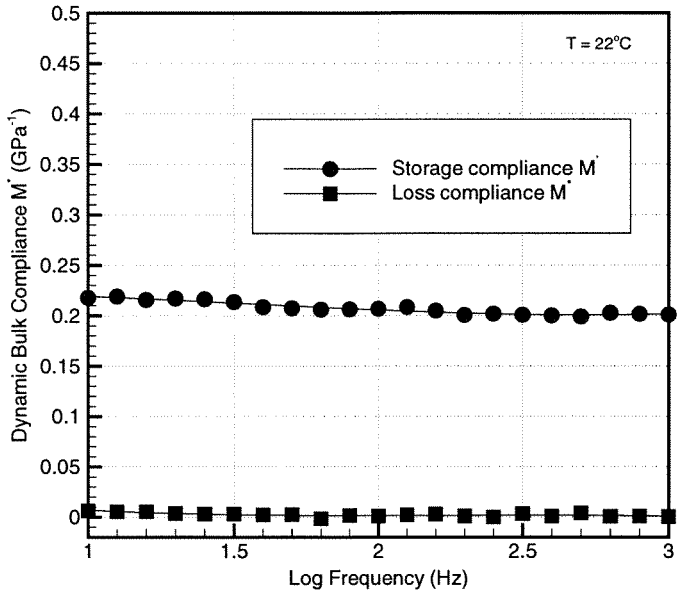

Figure 3.4: Storage compliance $M^{'}(f)$ and loss compliance $M^{''}(f)$ of PVAc at 22°C over two decades of frequency.

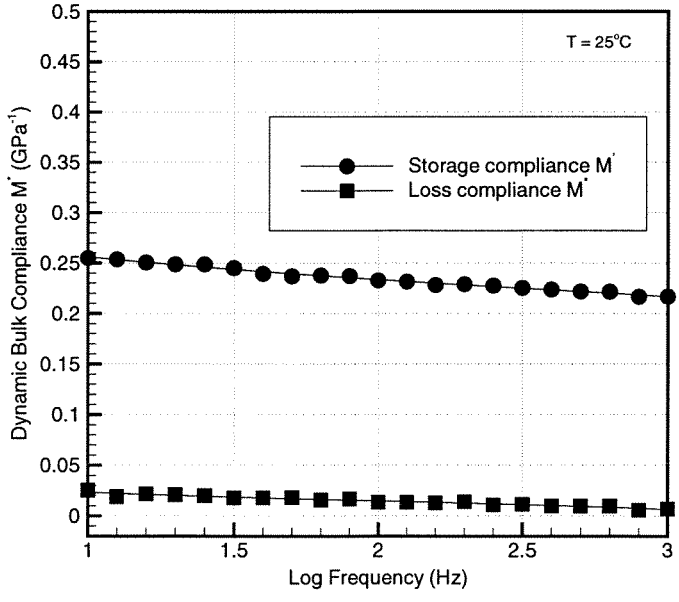

Figure 3.5: Storage compliance $M^{'}(f)$ and loss compliance $M^{''}(f)$ of PVAc at 25°C over two decades of frequency.

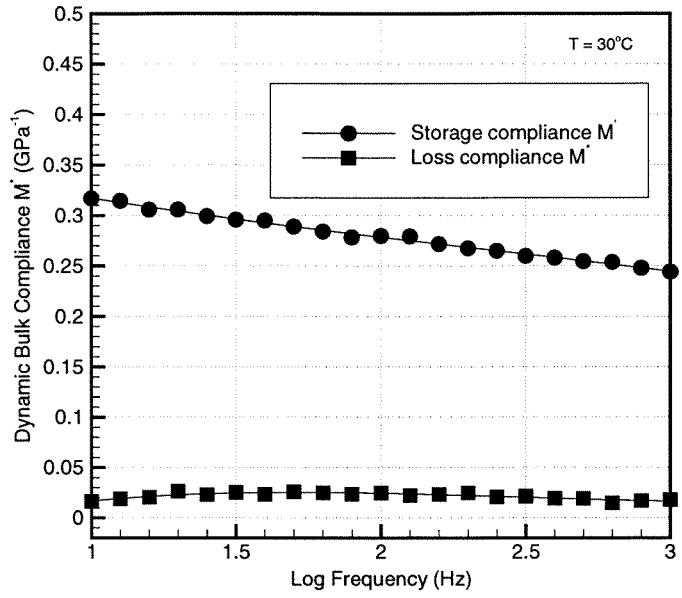

Figure 3.6: Storage compliance $M^{'}(f)$ and loss compliance $M^{''}(f)$ of PVAc at 30°C over two decades of frequency.

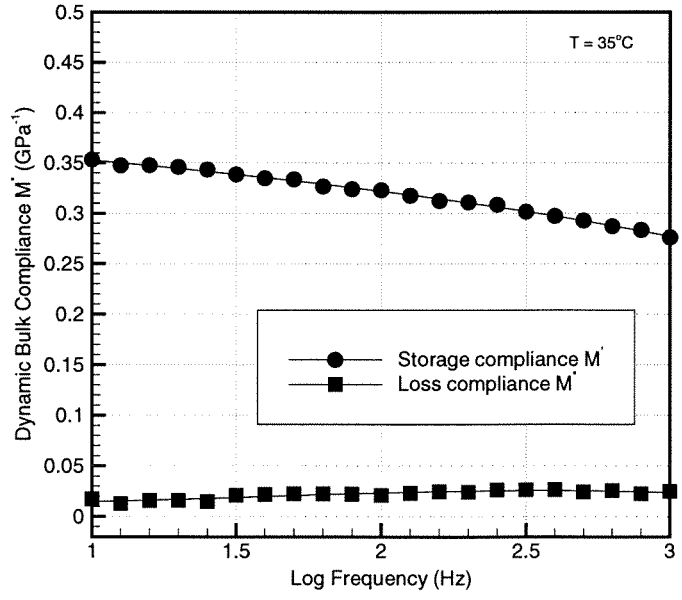

Figure 3.7: Storage compliance $M^{'}(f)$ and loss compliance $M^{''}(f)$ of PVAc at 35°C over two decades of frequency.

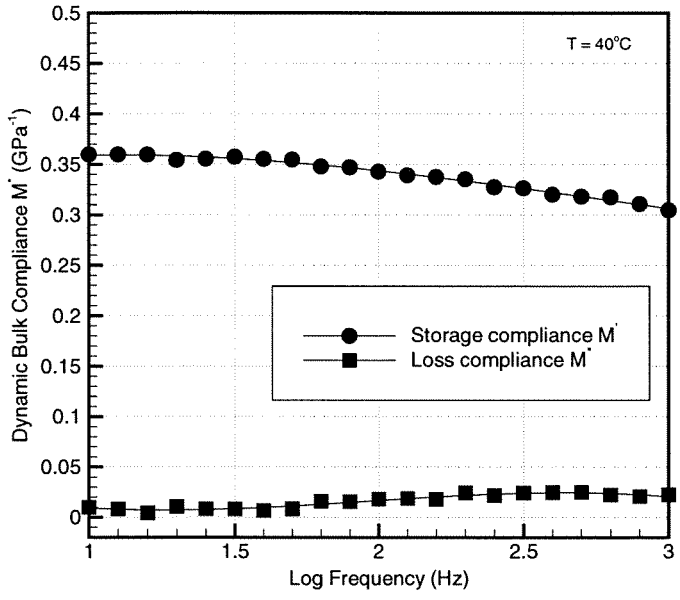

Figure 3.8: Storage compliance $M^{'}(f)$ and loss compliance $M^{''}(f)$ of PVAc at 40°C over two decades of frequency.

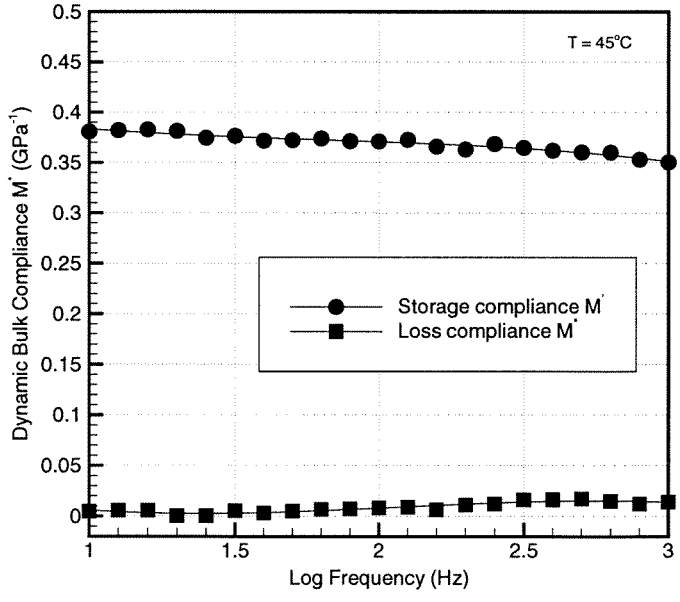

Figure 3.9: Storage compliance $M^{'}(f)$ and loss compliance $M^{''}(f)$ of PVAc at 45°C over two decades of frequency.

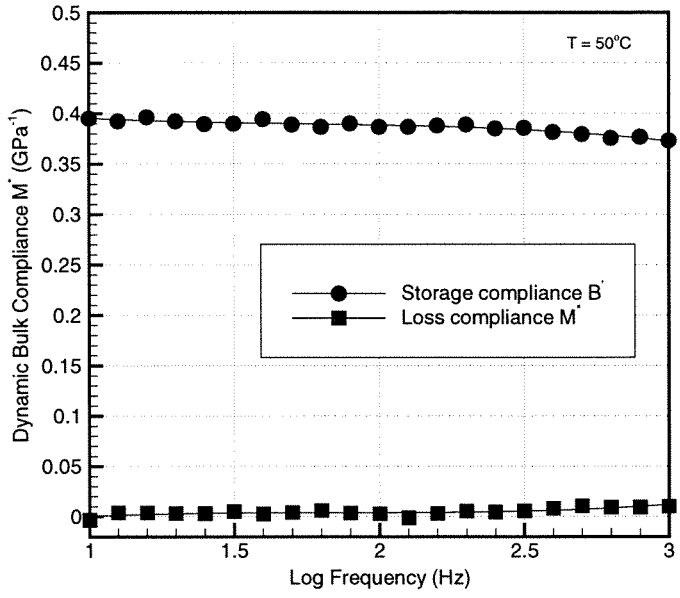

Figure 3.10: Storage compliance $M'(f)$ and loss compliance $M''(f)$ of PVAc at 50°C over two decades of frequency.

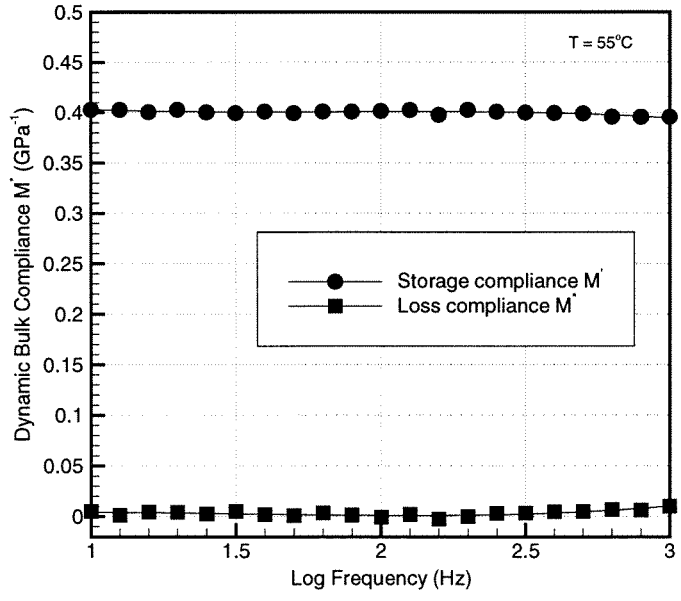

Figure 3.11: Storage compliance $M'(f)$ and loss compliance $M''(f)$ of PVAc at 55°C over two decades of frequency.

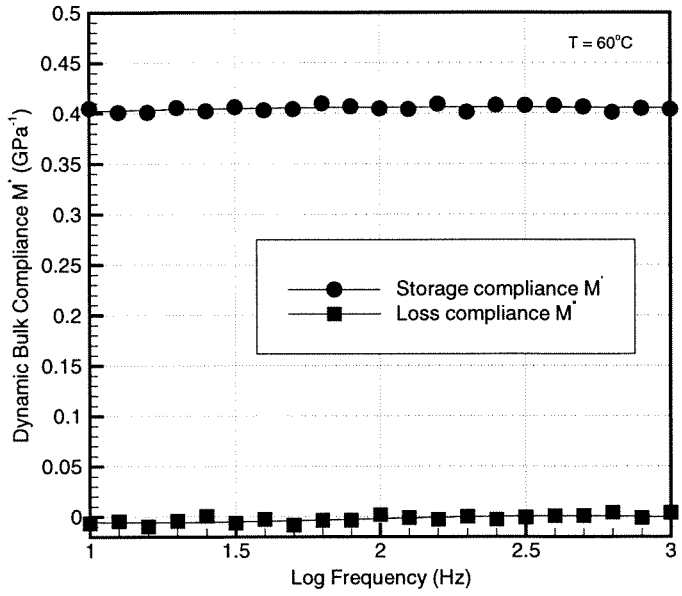

Figure 3.12: Storage compliance $M^{'}(f)$ and loss compliance $M^{''}(f)$ of PVAc at 60°C over two decades of frequency.

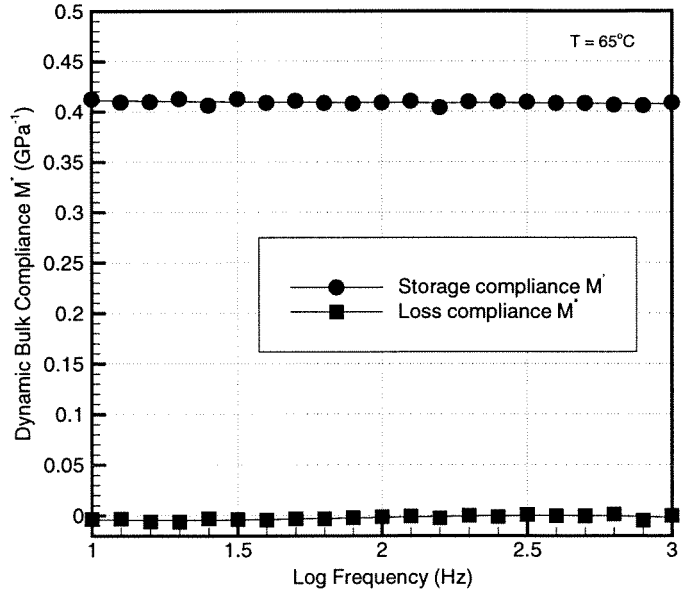

Figure 3.13: Storage compliance $M^{'}(f)$ and loss compliance $M^{''}(f)$ of PVAc at 65°C over two decades of frequency.

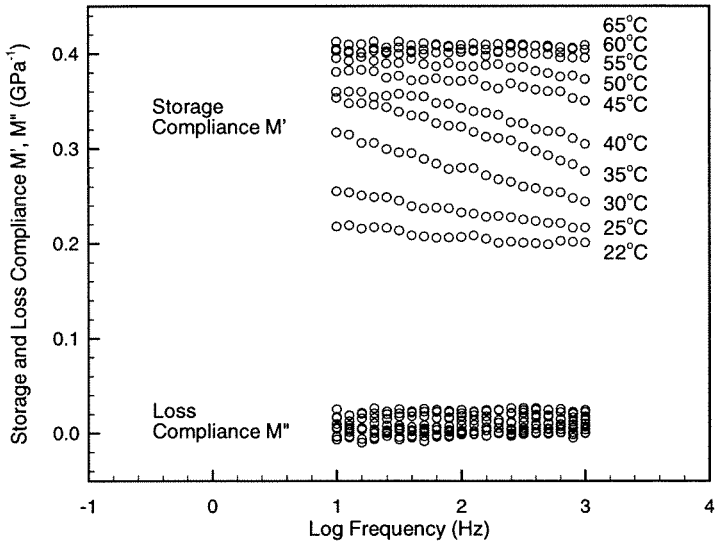

Figure 3.14: Storage compliance $M^{'}(f)$ and loss compliance $M^{''}(f)$ of PVAc at indicated temperatures over two decades of frequency.

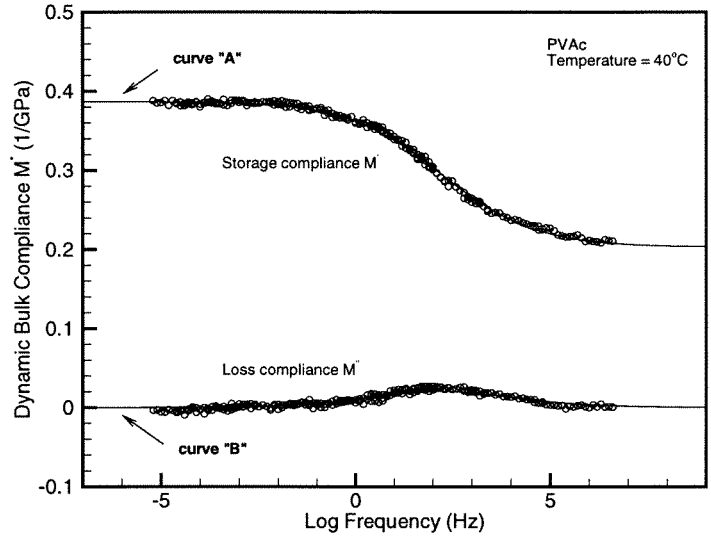

Figure 3.15: Master curves of storage and loss bulk compliances. Curve "A", fitted to the storage compliance was used to compute curve "B", the loss compliance. Corrections for rubber elasticity and thermal expansion are included.

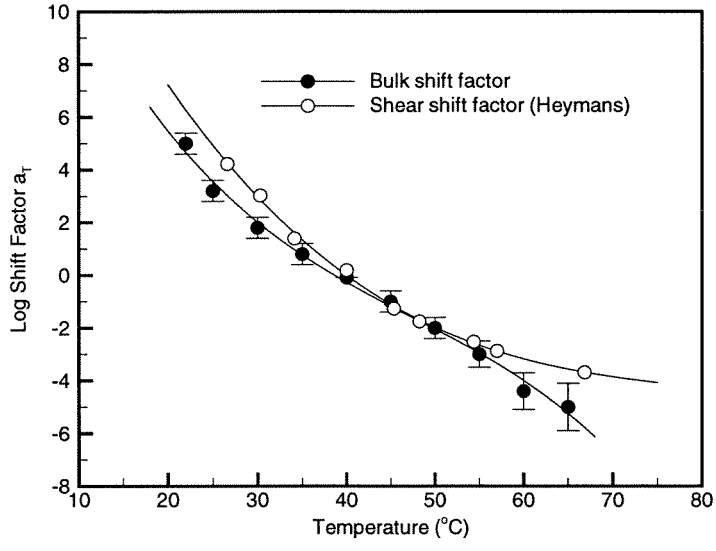

Figure 3.16: Bulk compliance shift factor comparison with shear modulus shift factor (Heymans, 1983).

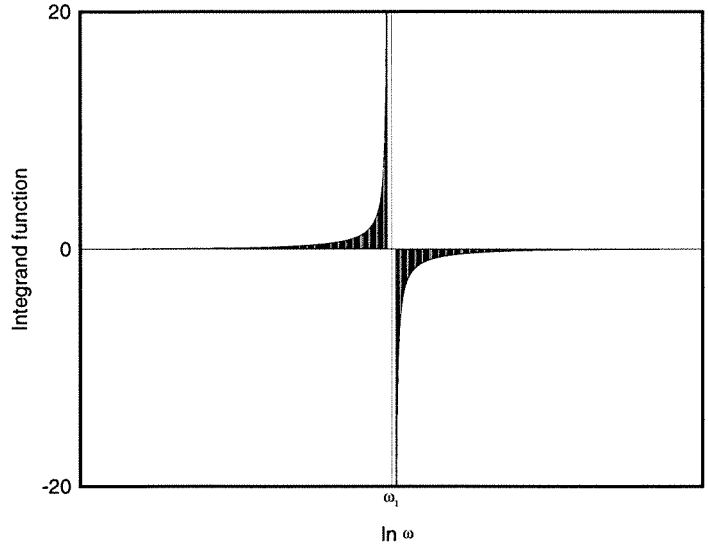

Figure 3.17: Integrand function in equation (3.2).

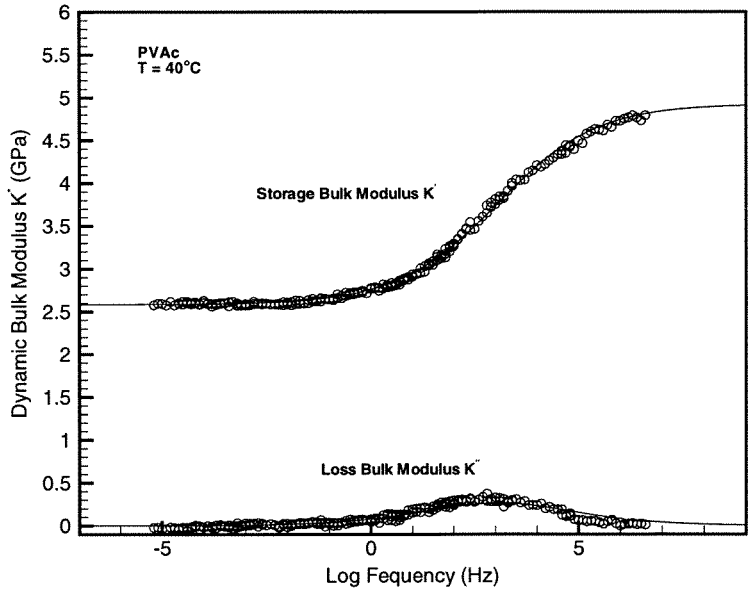

Figure 3.18: Master curves of storage and loss bulk moduli.

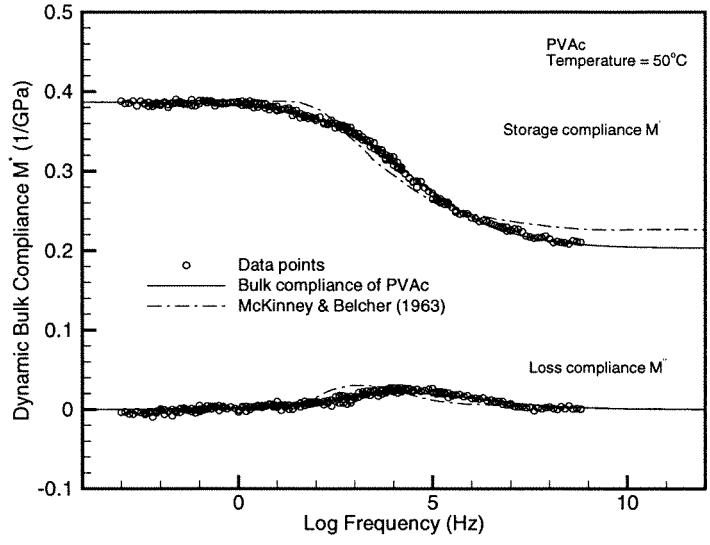

Figure 3.19: PVAc bulk compliance; comparison with McKinney and Belcher data.

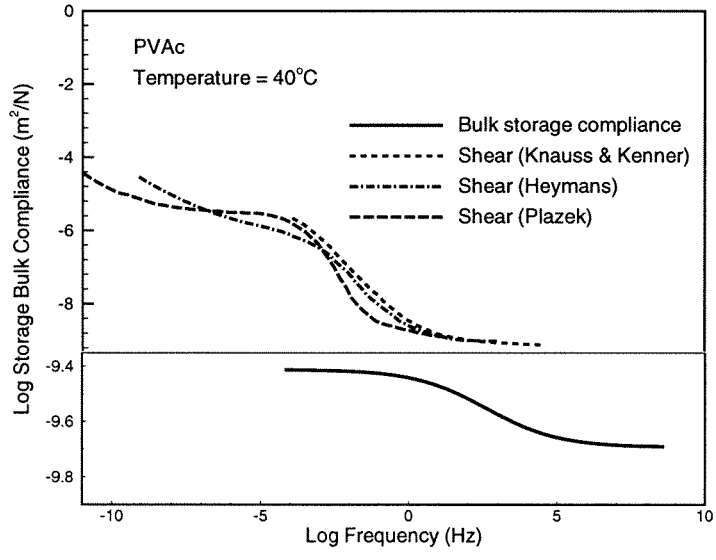

Figure 3.20: Comparison of shear and bulk compliances for PVAc. Knauss and Kenner, Heymans data for the same molecular weight PVAc (167,000) as for present study. Plazek's high molecular weight material has Mw = 650,000.

Chapter 4 Summaries

An computer-controlled automated system was designed and built for the measurement of dynamic bulk compliance of polymers. The device can measure the dynamic bulk compliance in the frequency range of more than two decades. The principle of design was based on a device developed by McKinney and Belcher, but the current apparatus covers a wider frequency range and provides a more accurate measurement by using digital lock-in amplifier and computer control. Different issues on how to increase the accuracy of the measurement were discussed.

The bulk compliance and modulus of a commercial sample of poly(vinyl acetate) [PVAc] was measured at frequencies from 10 to 1,000 Hz, temperature from 22°C to 65°C. It is confirmed that viscoelastic bulk response of PVAc under near infinitesimal deformations possesses a transition range separating its "glassy" and "rubbery" response. Although different versions of the same chemical material have been studied in the past, similar results have been obtained in that the ratio of the short-term to long-term response is about 1.9 as compared with a value of 2.6 for a material of similar molecular weight [Lin and Nolle, 1989] and 1.6 for the studies of McKinney and Belcher [1965] on a PVAc material not described any closer. This bulk response spectrum falls in essentially the time or frequency domain associated with the "glassy" shear response for this material. Apart from this mismatch the transition domains extend over roughly comparable time decades; this latter result is at variance with the findings of McKinney and Belcher on a seemingly different PVAc material.

The present results confirm thus that time or rate dependent deformations derive from different sources at the molecular level, which observation speaks for the mutual independence of the shear and bulk properties at infinitesimal deformations which underlie the linearized theory of viscoelasticity. The significant difference in the mean time of the transition ranges of the two material functions indicates that the molecular contributions to these two types of deformations mechanisms derive from different

chain and/or side-group mobilities. modulus is also much smaller than shear modulus because local movement of chain-like molecules needs less time than the long-range movement of molecules from each other. Based on parallel experimental studies, this independence appears to cease once larger than truly small deformations are involved, a first estimate for the boundary being projected for strains on the order of about 0.2%.

Future work includes increasing the temperature range for the measurement. Experiments are currently conducted from temperatures 0 to 20°C on the same PVAc material. Further studies will be on the testing of other material, for example, PMMA, which would require a higher temperature range (above 150°C). Two challenges facing the high temperature measurements are determining the bulk compressibility of the transmitting fluid and overcoming the lower voltage output from the piezoelectric transducers.

Appendix I Pressure Chamber Design

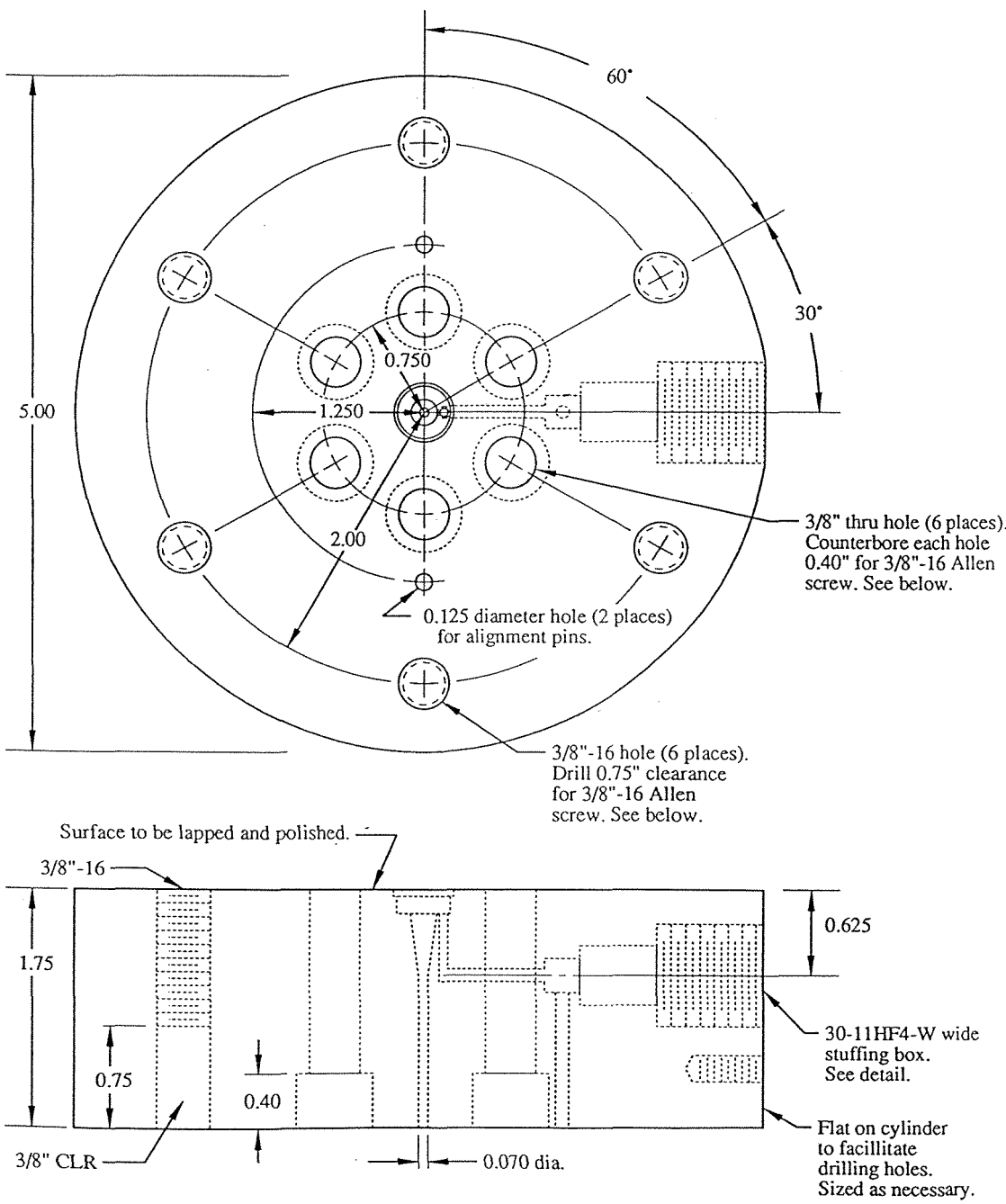

All dimensions in inches.

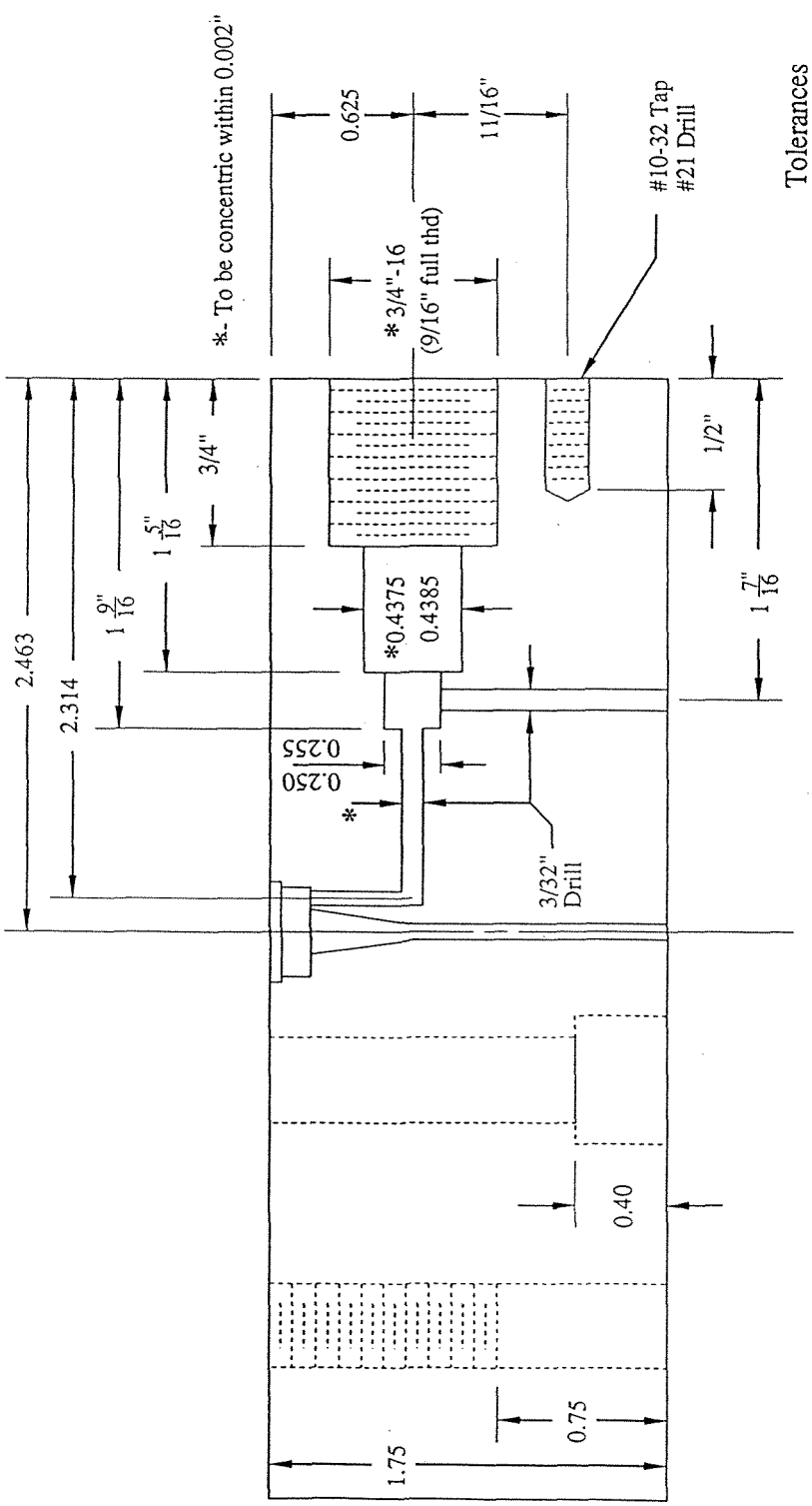

Tolerances
Fractional ± 1/64
.00 Decimal ± .010
.000 Decimal ± .005
Unless otherwise specified.

Note: This is an adaptation of the HiP 30-11HF4-W wide stuffing box for use with Grafoil packing for higher temperature.

Stuffing Box Detail

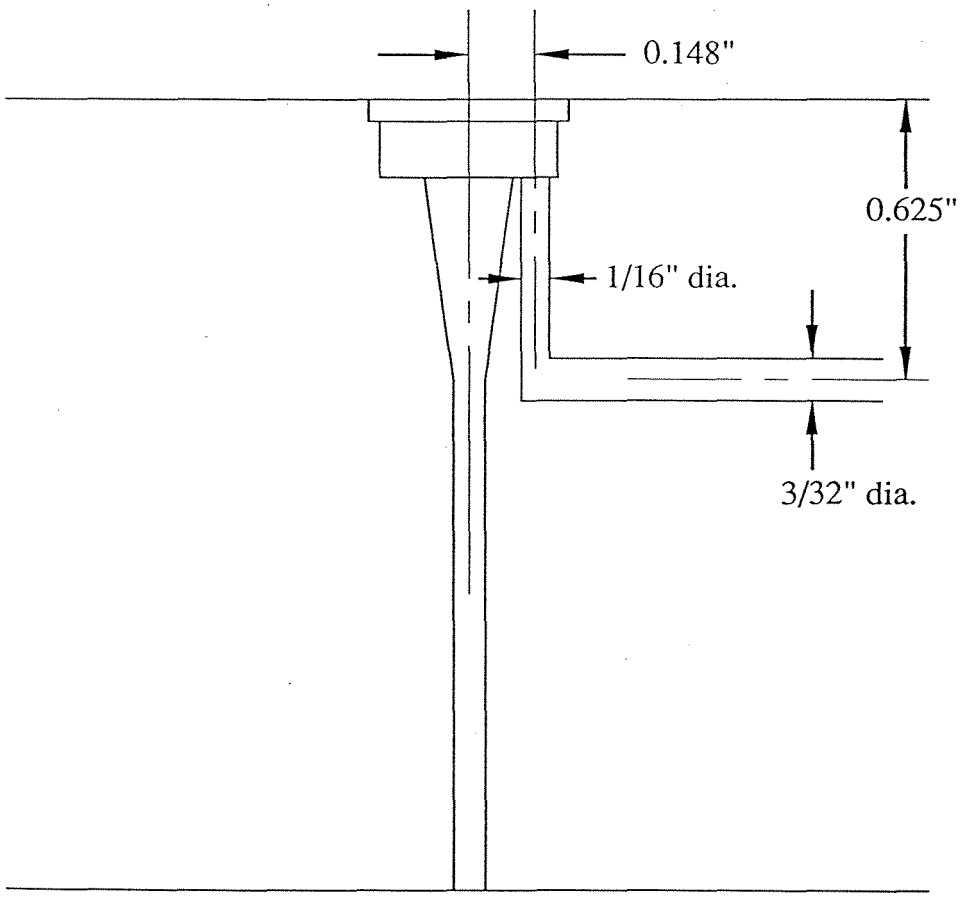

Oil Outlet Detail

Appendix II C Program to Calculate Dynamic Bulk Compliance

```
#include <stdio.h>
#include <stdlib.h>
#include <math.h>

void main(argc, argv)
int argc;
char *argv[];
{
        FILE *oil, *iron, *specimen, *out;
        char beep='\007';
        int i, index, ndata;
        float rc, ic, cr, ci, bc, bt, vc, vs, rd, id, dr, di, rb, ib, null;
        float freq[500], vpx[500], vpy[500], vox[500], voy[500], vix[500], viy[500],
              br[500], bi[500];

/* Check arguments: 1. number of argument; 2. input file name. */
  if(argc<5)
  {
        fprintf(stderr, "Usage: %s nospecimen calibration specimen out\n", argv[0]);
        fprintf(stderr, "Example: %s oil iron pvac out.dat\n", argv[0]);
        exit(1);
  }
  if((oil = fopen(argv[1], "r")) == NULL)
  {
        fprintf(stderr, "%c*** Can't open file %s\n", beep, argv[1]);
        exit(1);
  }
  if((iron = fopen(argv[2], "r")) == NULL)
  {
        fprintf(stderr, "%c*** Can't open file %s\n", beep, argv[2]);
        exit(1);
  }
  if((specimen = fopen(argv[3], "r")) == NULL)
  {
        fprintf(stderr, "%c*** Can't open file %s\n", beep, argv[3]);
        exit(1);
  }

/* Data input */
        /* Oil */
  index = 0;
  while((fscanf(oil, "%e%e%e%e%e", &freq[index], &vox[index], &voy[index], &null,
        &null)) != EOF)
  {
        index = index + 1;
  }
  ndata = index;
  fclose(oil);
        /* Iron */
  index = 0;
  while((fscanf(iron, "%e%e%e%e%e", &freq[index], &vix[index], &viy[index], &null,
                &null)) != EOF)
  {
        index = index + 1;
  }
  ndata = index;
  fclose(iron);
        /* Specimen */
  index = 0;
  while((fscanf(specimen, "%e%e%e%e%e", &freq[index], &vpx[index], &vpy[index],
        &null, &null)) != EOF)
  {
        index = index + 1;
  }
  ndata = index;
  fclose(specimen);

/* Material Constants */
  bc = 0.05987;
  printf("Bulk compliance of transimission fluid:\n");
  scanf("%f", &bt);
  printf("Volume of calibration sample:\n");
  scanf("%f", &vc);
  printf("Volume of specimen:\n");
  scanf("%f", &vs);
```

```
/* Calculate bulk compliance of the specimen. */
  for(index=0; index<ndata; index++)
  {
        rc = vox[index]/5.;
        ic = voy[index]/5.;
        cr = rc/(rc*rc + ic*ic);
        ci = ic/(rc*rc + ic*ic);
        rd = vix[index]/5.;
        id = viy[index]/5.;
        dr = (rd/(rd*rd + id*id) - cr)/(bc-bt)/vc;
        di = (id/(rd*rd + id*id) - ci)/(bc-bt)/vc;
        rb=vpx[index]/5.;
        ib = vpy[index]/5.;
        br[index]=bt+((rb/(rb*rb+ib*ib)-cr)*dr +
                (ib/(rb*rb+ib*ib)-ci)*di)/(dr*dr+di*di)/vs;
        bi[index]=((ib/(rb*rb+ib*ib)-ci)*dr -
                (rb/(rb*rb+ib*ib)-cr)*di)/(dr*dr+di*di)/vs;
  }

/* Output to file argv[4].  */
  if((out = fopen(argv[4], "w")) == NULL)
  {
        fprintf(stderr, "%c*** Can't open file %s\n", beep, argv[4]);
        exit(1);
  }
  for(index = 0; index < ndata; index++)
  {
        fprintf(out, "%e        %e      %e\n", freq[index], br[index], bi[index]);
  }
  fclose(out);
}
```

Appendix III Piezoelectric Transducer Output

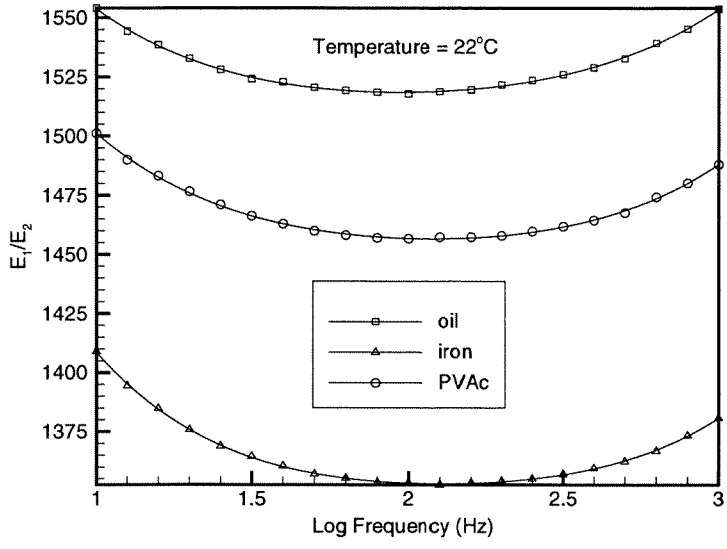

Figure 4.1: Input-output amplitude ratio (absolute value) , T=22°C

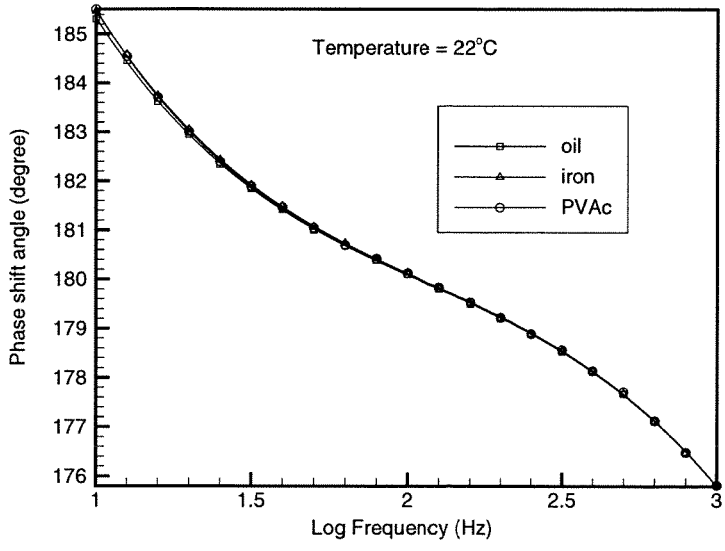

Figure 4.2: Phase shift angle between input and output piezoelectric transducers, T=22°C

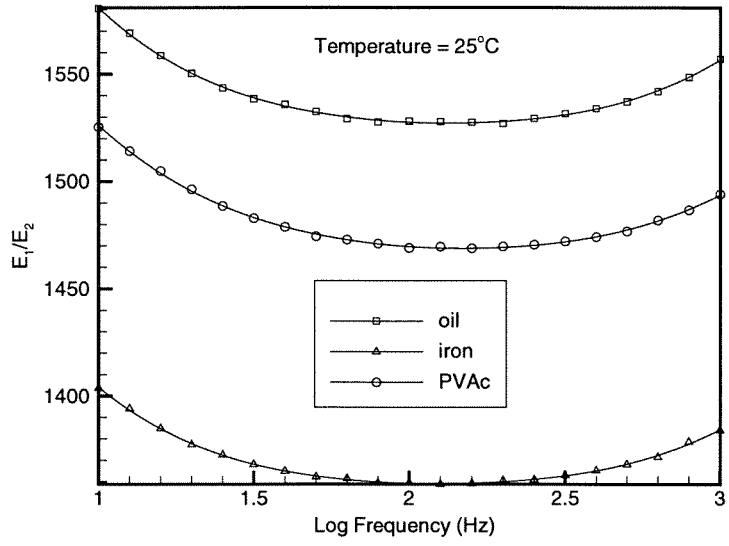

Figure 4.3: Input-output amplitude ratio (absolute value) , T=25°C

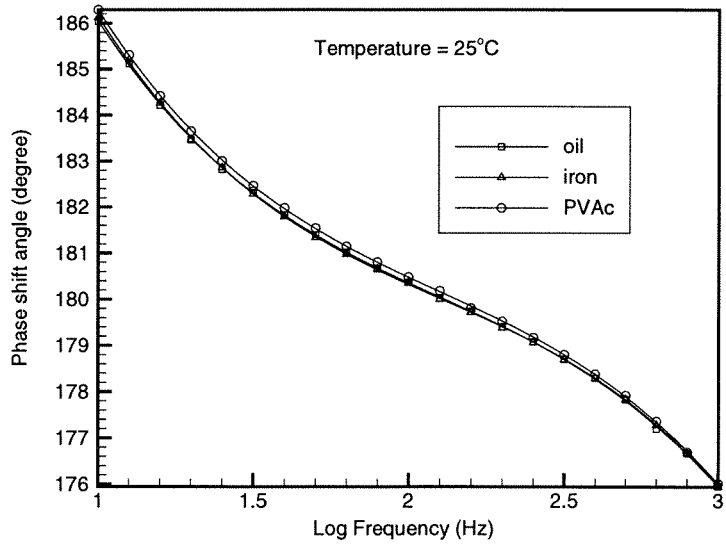

Figure 4.4: Phase shift angle between input and output piezoelectric transducers, T=25°C

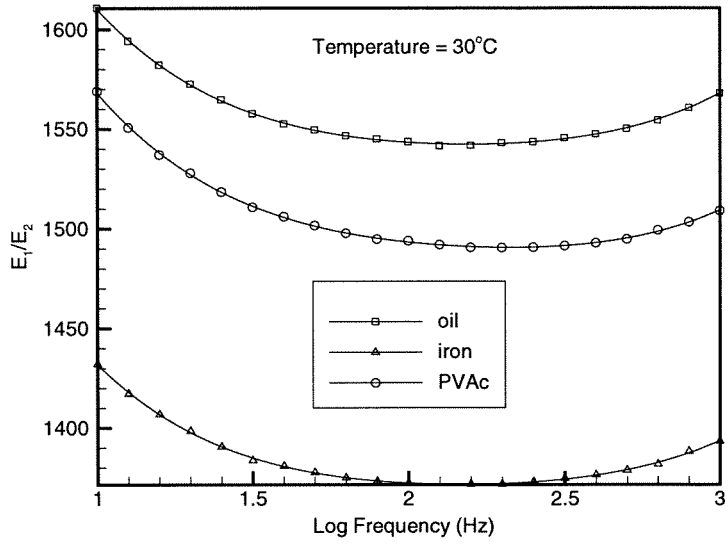

Figure 4.5: Input-output amplitude ratio (absolute value) , T=30°C

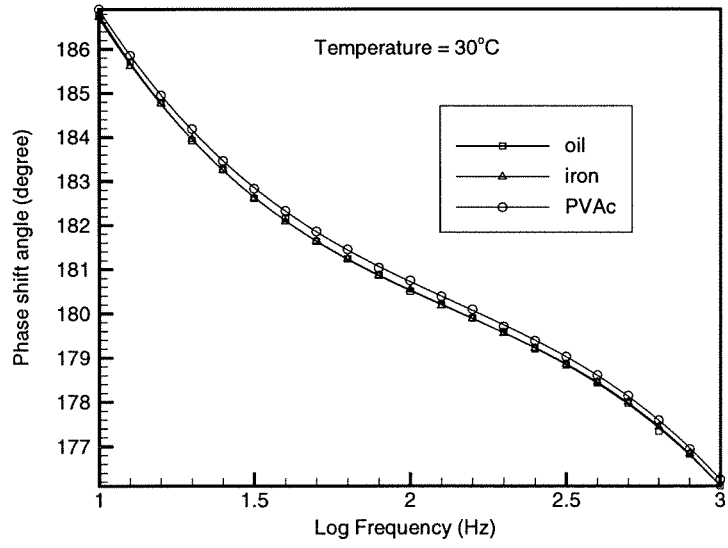

Figure 4.6: Phase shift angle between input and output piezoelectric transducers, T=30°C

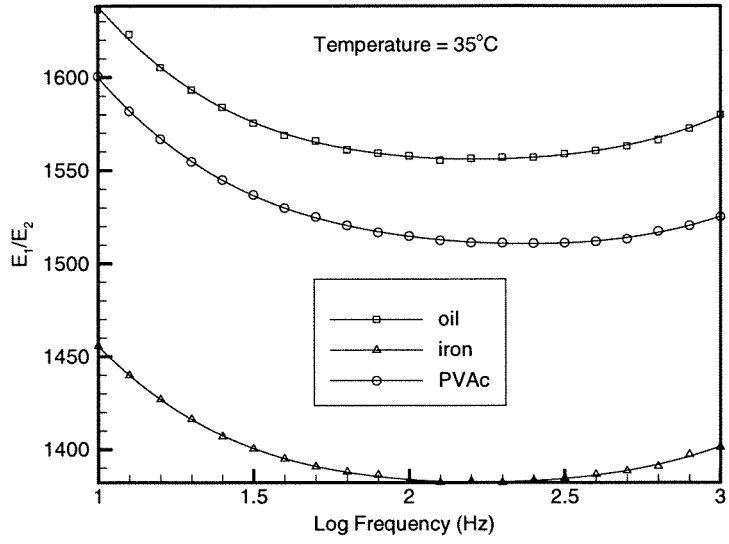

Figure 4.7: Input-output amplitude ratio (absolute value) , T=35°C

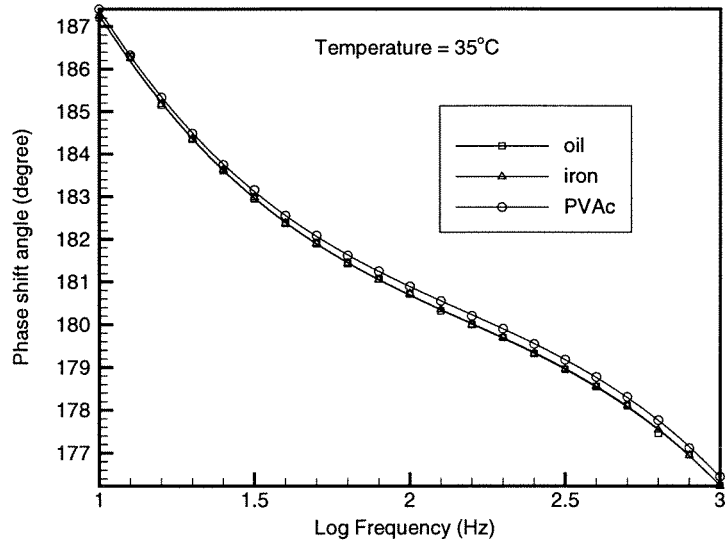

Figure 4.8: Phase shift angle between input and output piezoelectric transducers, T=35°C

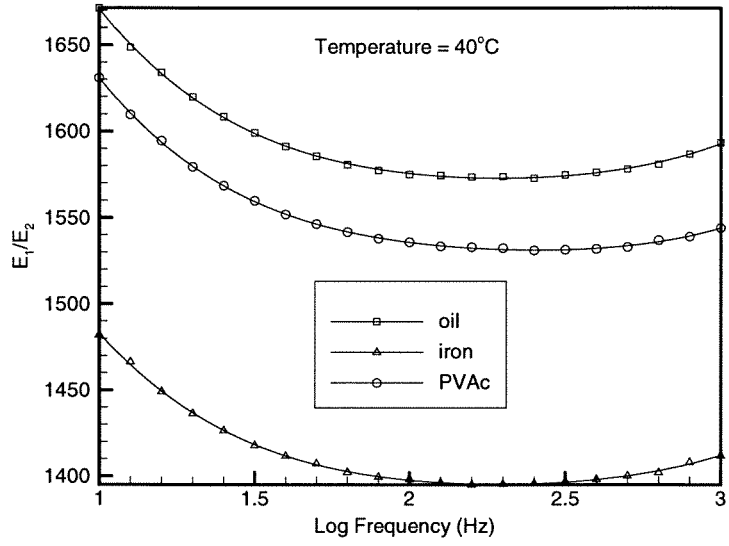

Figure 4.9: Input-output amplitude ratio (absolute value) , T=40°C

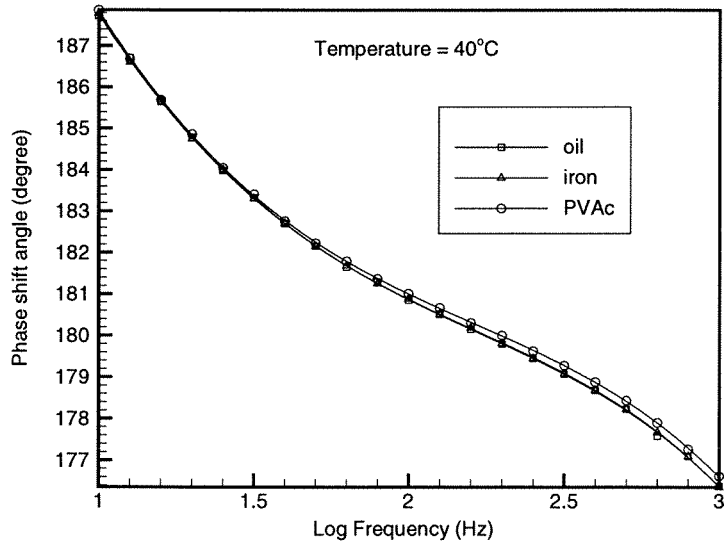

Figure 4.10: Phase shift angle between input and output piezoelectric transducers, T=40°C

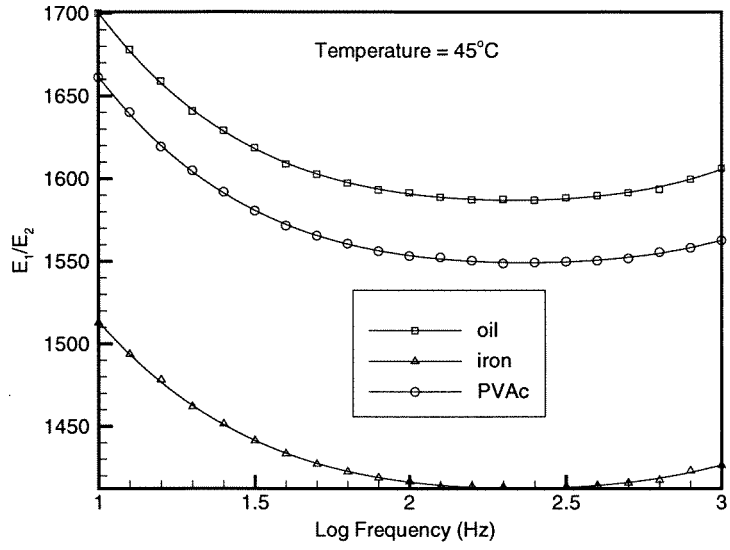

Figure 4.11: Input-output amplitude ratio (absolute value) , T=45°C

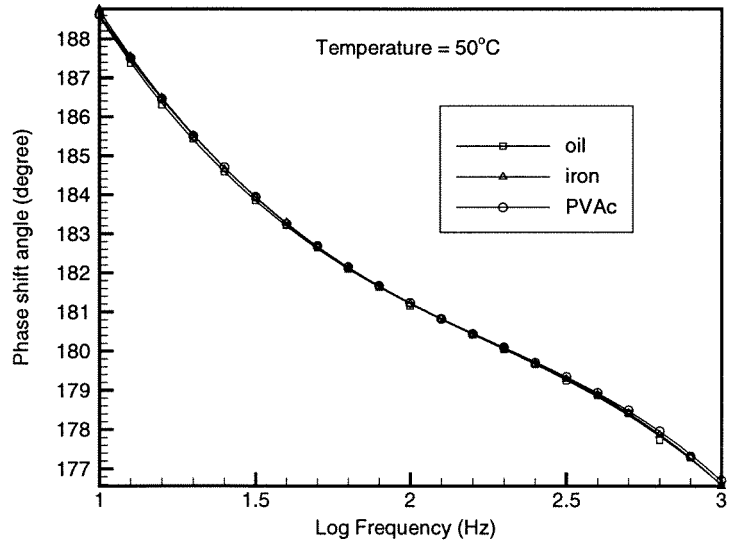

Figure 4.12: Phase shift angle between input and output piezoelectric transducers, T=45°C

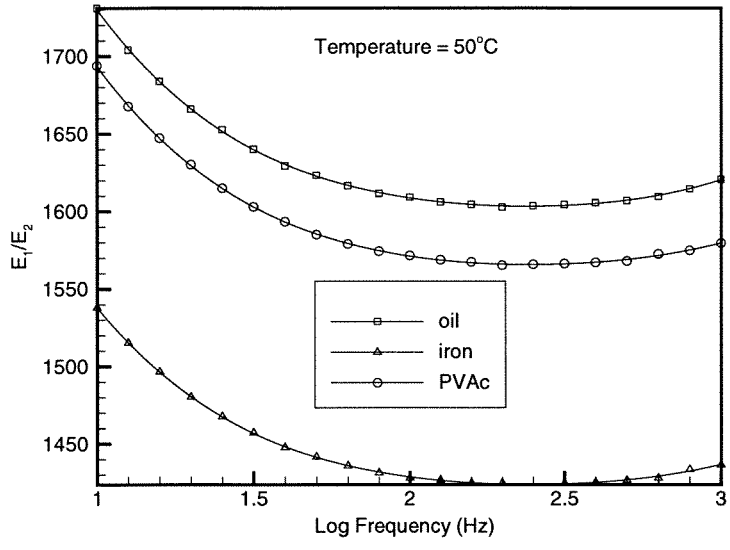

Figure 4.13: Input-output amplitude ratio (absolute value) , T=50°C

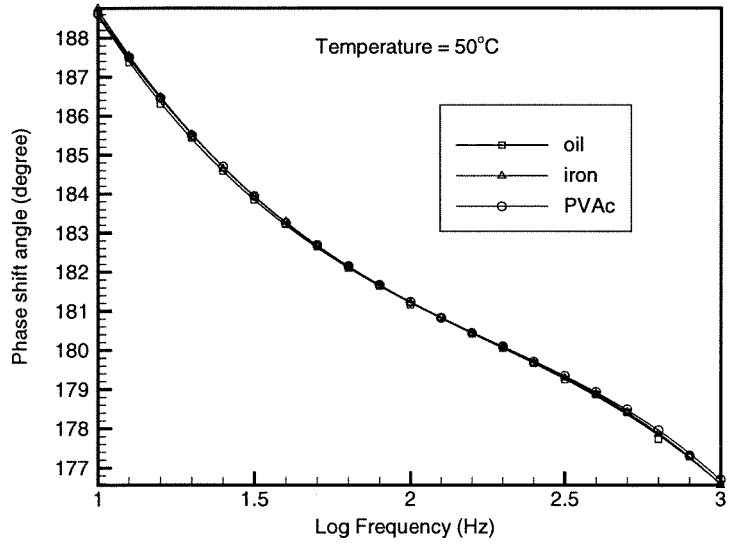

Figure 4.14: Phase shift angle between input and output piezoelectric transducers, T=50°C

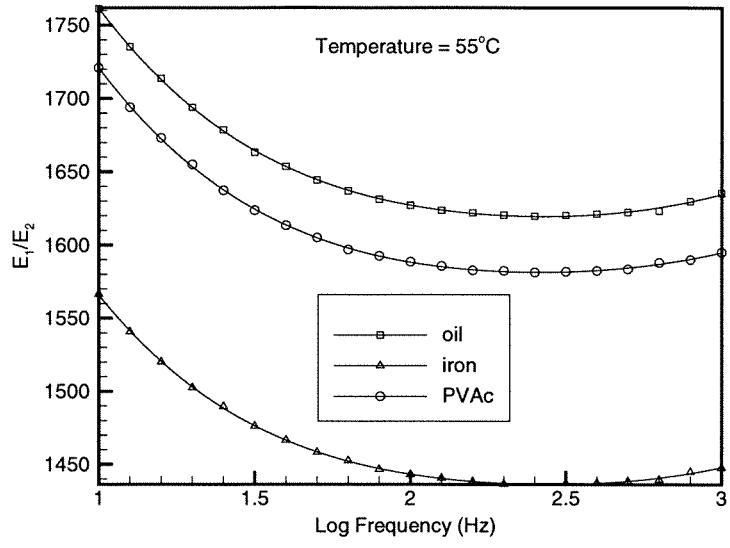

Figure 4.15: Input-output amplitude ratio (absolute value) , T=55°C

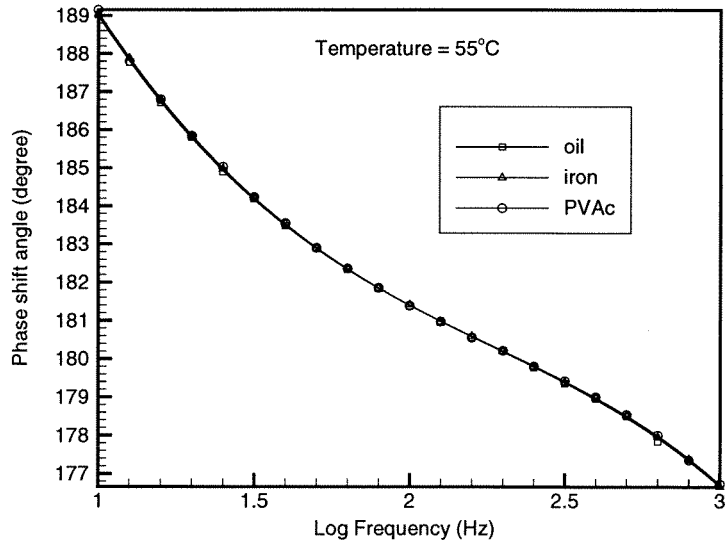

Figure 4.16: Phase shift angle between input and output piezoelectric transducers, T=55°C

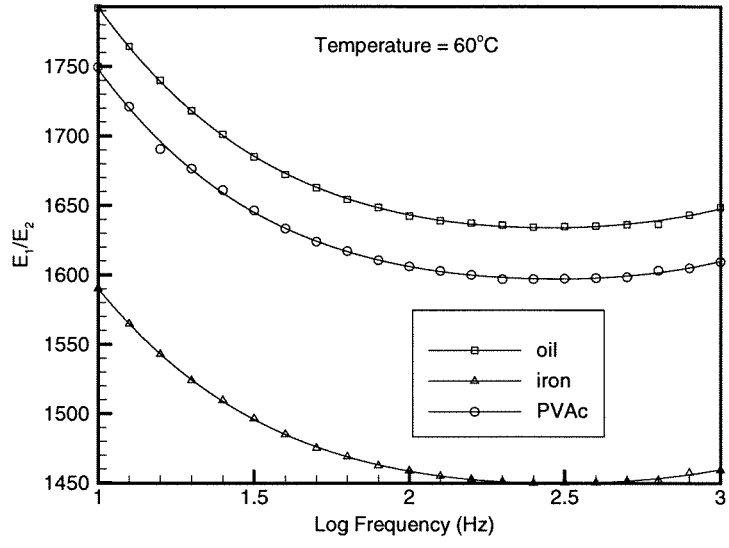

Figure 4.17: Input-output amplitude ratio (absolute value) , T=60°C

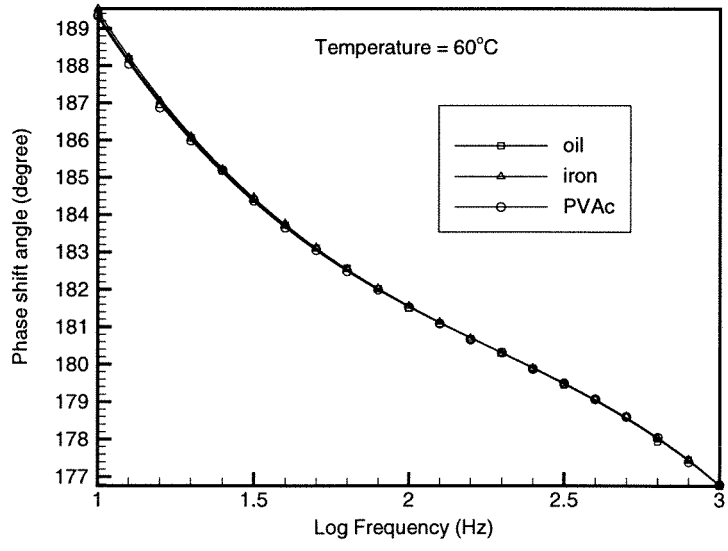

Figure 4.18: Phase shift angle between input and output piezoelectric transducers, T=60°C

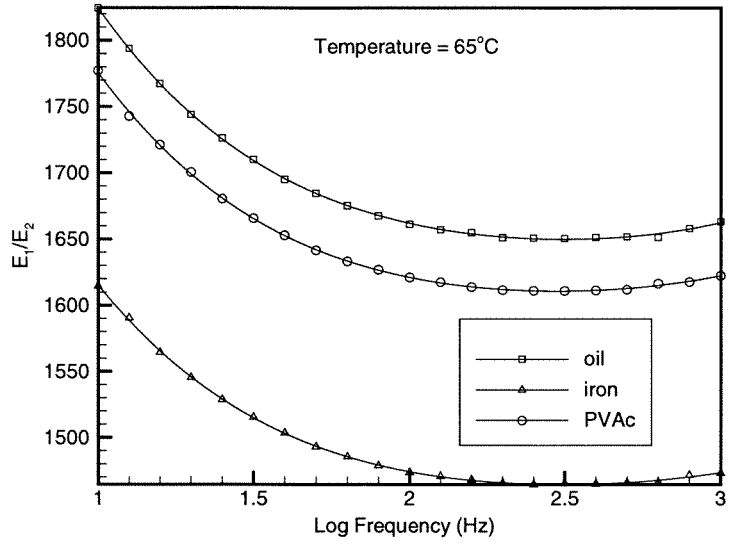

Figure 4.19: Input-output amplitude ratio (absolute value) , T=65°C

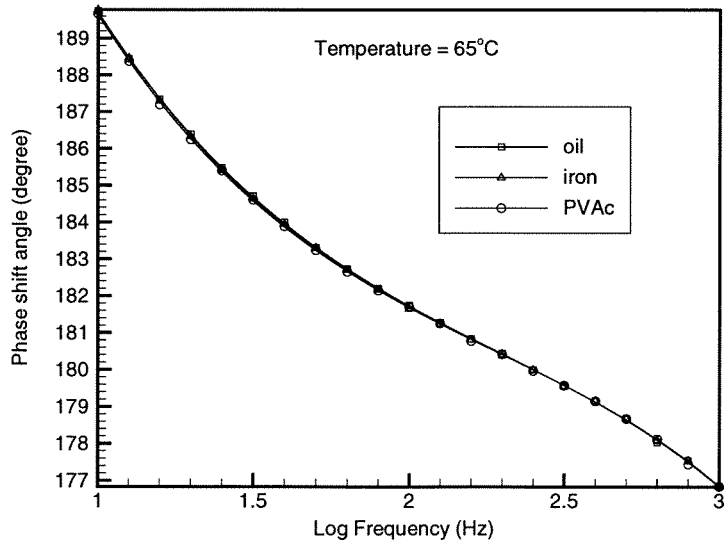

Figure 4.20: Phase shift angle between input and output piezoelectric transducers, T=65°C

Bibliography

Batchiski, A.J. (1913), *Z. Phys. Chem.*, **84**, 644.

Doolittle, A.K. and Doolittle D.B. (1957), *J. Appl. Phys.*, **28**, 901.

Doolittle, A.K. (1951), *J. Appl. Phys.*, **22**, 1471.

Duran, R.S. and McKenna, G.B. (1990), "A Torsional Dilatometer for Volume Change Measurements on Deformed Glasses: Instrument Description and Measurements on Equilibrated Glasses," *J. Rheology*, **34**, 813.

Ferry, J.D. (1980), *Viscoelastic Properties of Polymers*, 3rd Edition, Wiley, New York.

Fitzgerald, E.R. and Ferry, J.D. (1953), *J. Colloid Sci.*, **8**, 1.

Flugge, W. (1975), *Viscoelasticity*, 2nd Edition, Springer.

Heydemann, P. (1959), "The Dynamic Compressibility of Highpolymers in the Frequency Range from 0.1 c/s to 60 kc/s", *Acustica*, **9**, 446

Heymans, L.J. (1983), "An Engineering Analysis of Polymer Film Adhesion to Rigid Substrates", California Institute of Technology Ph.D. thesis.

Koppelmann, J (1955), *Kolloid-Z*, **144**, 12.

Knauss W.G., and Kenner, V.H. (1980), "On the Hygrothermomechanical Characterization of Polyvinyl Acetate", *J. Appl. Phys.*, **51**, 5131.

Knauss, W.G. and Emri, I.J. (1981), "Non-Linear Viscoelasticity Based on Free Vol-

ume Consideration", *GALCIT SM 80-11; Computers and Structures*, **13**, 123-128.

Knauss, W.G. and Emri, I.J. (1987), "Volume Change and the Non-Linearly Thermo-Viscoelastic Constitution of Polymers", *GALCIT SM 85-26; Polymer Engineering and Science*, A. Yee (ed.), **27**, 86-100.

Leaderman, H. (1943), "Creep of Filamentous Materials ", Textil Foundation, Washington, D.C.

Lin, T.S. and Nolle, A.W. (1989), "Dynamic Compressibility of Poly(Vinyl Acetate) and Poly(Methyl Methacrylate): Effects of Molecular Weight", *Polymer*, **30**, 648.

Losi, G.U. and Knauss, W.G. (1992), "Free Volume Theory and Nonlinear Thermoviscoelasticity", *GALCIT SM 90-22; Polymer Science and Engineering*, **32**, 542-557.

Lu, H. and Knauss, W.G. (1996), "Non-Linear Viscoelastic Behavior of PMMA Under Multiaxial Stress States", *GALCIT SM Report 96-6, to appear in Mech. Time Dep. Mat.*, Vol. **1**, Kluwer, Dordrecht, Netherlands.

Marvin, R.S. Aldrich, R. and Sack, H.S. (1954), *J. Apply. Phys.*, **25**, 1213.

Marvin, R.S. and McKinney, J.E. (1965), "Volume Relaxation in Amorphous Polymers, Physical Acoustics", *Physical Acoustics*, W.P. Mason (ed.), Vol. **IIB**, Academic Press, New York.

Matuooka, S (1960), *J. Polymer Sci.*, **42**, 511.

Matuooka, S (1962), *J. Polymer Sci.*, **57**, 569.

Matuooka, S. and Maxwell, B. (1958), *J. Polymer Sci.*, **32**, 131.

McKinney, J.E. and Belcher, H.V. (1963), "Dynamic Compressibility of Poly(Vinyl Acetate) and Its Relation to Free Volume", *J. Research of National Bureau of Stan-*

dards, A. Physics and Chemistry, **67A**, 43.

McKinney, J.E., Edelman, S. and Marvin, R.S. (1956), "Apparatus for the Direct Determination of the Dynamic Bulk Modulus", *J. Appl. Phys.*, **27**, 425.

Nolle, A.W. and Sieck, P.W. (1952), *J. Appl. Phys.*, **23**, 888.

Philippof W. and Brodnyan (1955), *J. Appl. Phys.*, **26**, 846.

Plazek, D.J. (1980), "The Temperature Dependence of the Viscoelastic Behavior of Poly(vinyl acetate)", *Polymer Journal*, **12**, 43.

Tobolsky, A.V. and Andrews, R.D. (1943), *J. Chem. Phys.*, **11**, 125.

Treloar, L. R. G. (1949), "The Physics of Rubber Elasticity", Oxford University Press (Clerendo), London and New York.

Trent, H. M (1948), "The Absolute Calibration of Electro-Mechanical Pickups", *J. Appl. Mech., Trans. Am. Soc Mech. Engrs.*, **70**, 49.

Turnbull, D. and Cohen, M.H. (1961), *J. Chem. Phys.*, **34**, 120.

Wada, Y., Hirose, H., Asano, T and Fukutomi, S (1959), *J. Phys. Soc. Jpn.*, **14**, 1064.

Waterman, H. A. (1963), "Determination of the Complex Moduli of Viscoelastic Materials with the Ultrasonic Pulse Method", *Kolloid-Z*, **192**, 1.

Williams, M.L., Landel, R.F. and Ferry, J.D. (1955), *J. Am. Chem. Soc.*, **77**, 3701.